Carbonate Clumped Isotope Thermometry of Bulk Planktonic Foraminifera

Matthew Goldklang
Mark Pagani and Pincelli Hull
May 6th 2016

A Senior Thesis presented to the faculty of the Department of Geology and Geophysics, Yale University, in partial fulfillment of the Bachelor's Degree.

Abstract:

The use of carbonate-clumped isotope thermometry (Δ_{47}) is gaining traction in paleoclimate reconstruction for its relatively strict thermodynamic control. Much work is being done on determining accurate calibrations, both for biogenic and inorganic carbonates. Clumped-carbonate thermometry shows increasing promise through such calibrations for reconstructing sea surface temperature (SST) with planktonic foraminifera, but discrepancies arise with different laboratory techniques and instrumentation. In addition, obtaining enough material of a certain species of planktonic foraminifera limits the applicability of these abundant microfossils in paleoclimate work. This study aims to reduce these complications by analyzing modern bulk planktonic foraminifera from three core tops to test if picking out specific species is necessary. The core top Δ_{47} results are fitted to the calibrations presented by Zaarur et al. 2013 compared to the monospecific results presented in previous studies (Tripati et al., 2010; Grauel et al., 2013). The bulk planktonic foraminifera fit the calibration within the same error as the monospecific foraminifera results, with no constraints on the used size fraction. After calibrating bulk planktonic foraminifera to the carbonate-clumped isotope thermometer, we apply the technique to planktonic foraminifera from the Eocene. The use of bulk planktonic foraminifera in future paleo-SST reconstruction will reduce time and measurement restrictions associated with preparing samples.

One Sentence Summary: Bulk planktonic foraminifera fit the carbonate clumped isotope calibration discussed in Zaarur et al. (2013) just as well as previous monospecific analyses.

1.0 Introduction:

1.1 Clumped Isotope Thermometry

Paleoclimate records are vital for understanding the future of the climate system. As humans continue to emit CO_2 into the atmosphere, it is crucial to constrain the magnitude that the Earth will warm and the consequential large-scale changes in global climate patterns. Paleoclimate data inform climate models and provide insight into how the Earth system has responded to climatic changes of the past.

The most common proxy for determining paleoclimatic conditions is the oxygen isotope ($\delta^{18}O$) value in carbonates, specifically that of shelled marine organisms. Oxygen exists in three stable isotopes: ^{16}O, ^{17}O and ^{18}O. $\delta^{18}O$ paleothermometry is based on the temperature dependence of the fractionation between lighter, more common oxygen isotope (^{16}O), and the heavier, more rare isotope (^{18}O). The oxygen isotope signature of marine organisms records the $\delta^{18}O$ of seawater and an associated, often species-specific, temperature-dependent offset. Thus, trying to extract temperature data from oxygen signatures requires an assumption of the $\delta^{18}O$ of seawater. There is a lot of uncertainty in assuming the $\delta^{18}O$ of seawater. The signal relies on global ice volumes, salinity, terrestrial inputs, and the hydrological cycle. To isolate $\delta^{18}O_{seawater}$ from the temperature offset of carbonate precipitation, novel proxies are necessary to constrain temperature. Geochemists have developed inorganic trace metal proxies for the tests of marine organisms, specifically the Mg/Ca – temperature proxy (Nürnberg, 2000; Lea et al., 2002), but these require precise knowledge of seawater composition and salinity in context of the proxy to accurately calculate temperature. Additionally, studies have shown relationships between organic lipid compositions to seawater temperature (e.g. Brassell et al., 1986; Schouten et al., 2002). These proxies, however, often are associated with poorly understood biology.

Carbonate clumped isotope analysis is an emerging proxy for paleoclimate reconstruction with enormous potential for recording and isolating past temperature. Represented by Δ_{47}, the proxy is based on the bond between the two rare, heavy isotopes, ^{13}C-^{18}O, within the carbonate mineral lattice (Ghosh et al. 2006ab; Affek, 2012; Eiler, 2007; Guo et al., 2009). It reflects the internal ordering of the bonds within carbonate's crystal structure. The clumping of the two

heavy atoms, forming the heavy isotopologue, is a consequence of slight differences in vibrational energy of all possible isotopologues. A bond containing one heavy isotope is 'stronger' than a bond containing none, and a bond containing two heavy isotopes is stronger than a bond containing one (Affek, 2012). Thus theory predicts that the clumping reaction, depicted below, is thermodynamically controlled, and it occurs at equilibrium within the crystal lattice. With increasing temperature, a forming carbonate crystal will have a more random distribution of heavy isotopes among isotopologues because the ground state energy differences among the isotopologues diminish. The ratio of the heavy isotopologue, conversely, increases with lower temperatures. The signal is distinct from the separate $\delta^{18}O_{carbonate}$, which depends on the $\delta^{18}O_{seawater}$ and temperature, and is distinct from $\delta^{13}C$ values, which are controlled by dissolved inorganic carbon (DIC). The Δ_{47} proxy measures the excess of the heavy isotopologue, $^{13}C^{18}O^{16}O$, with a mass of 47 amu, relative to the most abundant isotopologue, $^{12}C^{16}O^{16}O$, with a mass of 44 amu (Affek, 2012).

$$X^{12}C^{18}O^{16}O_2 + X^{13}C^{16}O_3 \rightarrow X^{13}C^{18}O^{16}O_2 + X^{12}C^{16}O_3$$

Equation 1 depicts the internal isotope exchange within a carbonate mineral, where X is a cation (Ca^{2+} or Mg^{2+}). The K_{eq} of the reaction approaches 1 with increasing temperature (Tripati et al., 2015).

$$\Delta_{47} = \left[\frac{R^{47}}{2R^{13} \times R^{18} + 2R^{17} \times R^{18} + R^{13} \times \left(R^{17}\right)^2} - \frac{R^{46}}{2R^{18} + 2R^{13} \times R^{17} + \left(R^{17}\right)^2} - \frac{R^{45}}{R^{13} + 2R^{17}} + 1 \right] \times 1000$$

Equation 2, of Affek (2012), determines the excess mass 47 isotopologue over that expected from a random distribution.

1.2 Calibrations and Applications

Because the ordering of the bonds is internal and thermodynamically controlled, the predicted relationship between Δ_{47} and temperature can be applied in a variety of settings, both marine and terrestrial, and applied to both biogenic and inorganic materials. Many have aimed to constrain paleoclimatatic conditions (Finnegan et al., 2011, Eiler, 2011, Affek et al., 2008).

Before doing so, it necessary to constrain the Δ47-temperature relationship. Numerous calibrations have been calculated, the first being for inorganic calcite precipitation and coral growth in laboratory settings (Ghosh et al. 2006a). The Ghosh et al. (2006a) calibration measured the Δ_{47} signal from synthetic calcites digested in phosphoric acid compared to the precipitation temperature, without the use of standards (see Equation 3 below). This calibration, with additional data and retroactive application of standards, is the most widely used Δ_{47} – temperature relationship to date (e.g., Zaarur et al., 2013; Eagle et al., 2011; Tripati et al., 2010).

$$\Delta_{47} = 0.0592 \text{ X } 10^6 / T^2 - .02$$

Equation 3 Describes the original calibration presented in Ghosh et al. (2006a) for temperatures between 1 and 50 °C.

Other studies have found different calibrations to account for varying precipitation and digestion methods, and observed biogenic temperature-Δ_{47} relationships (eg., Dennis and Schrag 2010, Zaarur et al., 2013, Tripati et al., 2015). Most of the variability among differing calibrations can be attributed to digestion technique. Carbonate, for clumped analysis, is most commonly digested in phosphoric acid, which produces a predictable fractionation. The fractionation, however, is different at different temperatures. Studies that follow the techniques first developed by Ghosh et al. (2006a) digest their samples in 25°C, and often overnight. Other

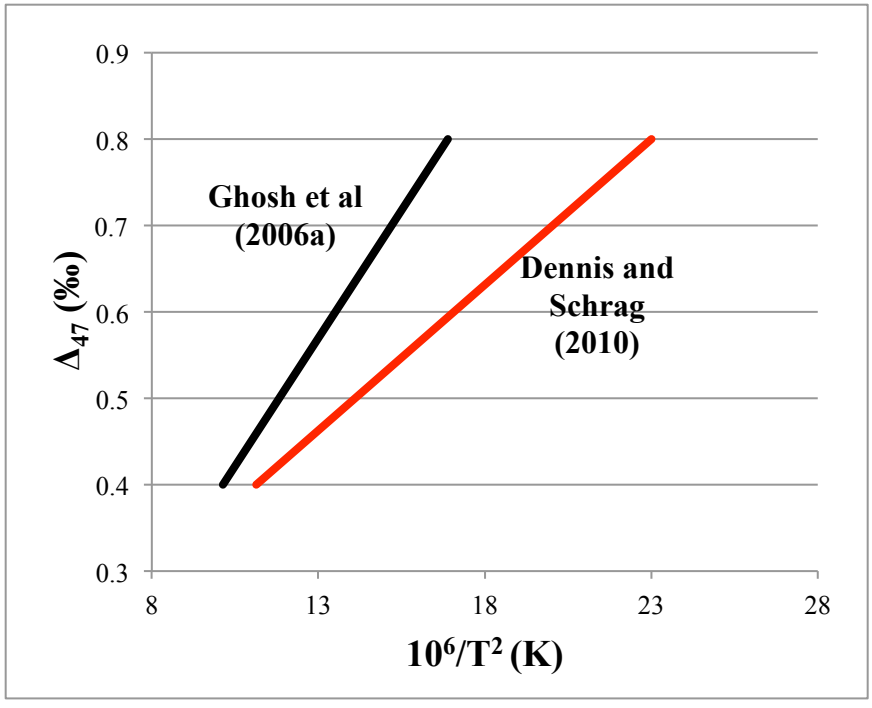

Figure 1 depicts the differences in fractionation between acid digestion, using phosphoric acid, at 25°C and 90°C. Increasing the temperature of digestion shallows the slope of the calibration. The black line is the calibration presented in Ghosh et al. (2006a) and the red line corresponds with the calibration presented in Dennis and Schrag (2010).

studies (e.g., Dennis and Schrag, 2010) digest the carbonates at 90°C, resulting in a calibration with a shallower slope with a larger intercept (Figure 1). Moreover, procedures for samples and standards vary per laboratory leading to difficult comparisons among studies. Dennis (2007) developed an absolute reference frame through incorporating standard calibration from varying laboratories, for both digestion methods. Much of the existing data for Δ_{47}-temperature calibrations and applications still exists in the Ghosh et al. (2006a) frame, but there is increasing effort to report the absolute reference frame. In this study, we will present the data in the absolute reference frame, but will then analyze the data as in Ghosh et al. (2006a) for ease of comparison to previous studies.

Study	Source Carbonate	Biogenic Source (if applicable)	Reference Frame	Digestion Temperature (°C)	Calibration
Ghosh et al (2006a)	Synthetic and Biogenic	Corals	Ghosh et al (2006a)	25	$\Delta_{47}= (0.0592)10^6/T^2$ -.2
Dennis and Schrag (2010)	Synthetic and Inorganic	NA	Dennis and Schrag (2010)	90	$\Delta_{47}= (0.0337\pm 0.0018)10^6/T^2 +(0.2470\pm 0.0194)$
Dennis et al. (2011)	Synthetic and Inorganic	NA	Absolute	90	$\Delta_{47}= (0.0362\pm 0.0018)10^6/T^2 + (0.2920\pm 0.0194)$
Dennis et al. (2011)	Inorganic and Biogenic	Corals (used data from Ghosh)	Absolute	25	$\Delta_{47}= (0.0636\pm 0.0049)10^6/T^2 - (0.00047\pm 0.0520)$
Tripati et al. (2010)	Synthetic and Biogenic	Foraminifera	Ghosh et al (2006a)	25	$\Delta_{47}= (0.05875\pm 0.00133)10^6/T^2 - (0.0140\pm 0.1384)$
Grauel et al. (2013)	Biogenic	Foraminifera	Ghosh et al (2006a)	25	$\Delta_{47}= (0.050581\pm 0.007)10^6/T^2 - (0.0807\pm 0.0079)$
Zaruur et al. (2013)	Inorganic and Biogenic	Corals, Coccoliths, Foraminifera, Molluscs, Brachiopods, Otoliths	Absolute	25	$\Delta_{47}= (0.0555\pm 0.0027)10^6/T^2 + (0.0780\pm 0.0298)$
Zaruur et al. (2013)	Ibid	Ibid	Ghosh et al (2006a)	25	$\Delta_{47}=(0.0526\pm0.0025)\times10^6/T^2 +(0.0520\pm0.0284)$
Tang et al. (2014)	Synthetic	NA	Absolute	100	$\Delta_{47}= (0.0387\pm 0.0072)10^6/T^2 + (0.2532\pm 0.0289)$
Kluge et al. (2015)	Synthetic	NA	Absolute	90	$\Delta_{47}= (0.0380\pm 0.07)10^6/T^2 + (0.259\pm 0.006)$
Tripati et al. (2015)	Synthetic, Biogenic, and Inorganic	Corals	Ghosh et al (2006a)	90	$\Delta_{47}= (0.0460\pm 0.0034)10^6/T^2 + (0.1649\pm 0.0786)$

Table 1 presents the relevant, calculated Δ_{47}-temperature calibrations to date.

Several studies have tested, and some have revised, the above calibrations using a variety of carbonate precipitating organisms (Table 1). Large, carbonate preciptating organisms or large inorganic carbonates tend to be the most applied because of the large sample size requirements for analytical precision. Ghosh et al. (2007) analyzed fish otoliths, which when assuming the growth temperature of the fish, closely matched their previously founded calibration. Analysis of

teeth bioapatite from mammals (Eagle et al., 2010) was also found to match the Ghosh et al., (2006a) calibration, which was then applied to understand Pleistocene mammal dynamics. Most studies dealing with carbonate forming macrofauna (mollusks, brachiopods, and corals) have found slightly shallower slopes or large deviations from the calibration for specific species (Henkes et al., 2013; Eagle et al., 2013; Saenger et al., 2012), except for one study, Thiagarajan et al. (2010), which presents results that match the Ghosh et al. (2006a) calibration for shallow water corals. Some attribute such discrepancies to isotopic mixing and kinetic effects that occurs during the specific, slow biomineralization processes (Tang et al., 2014). Furthermore, large organisms are not evenly distributed across the world and offer a limited perspective on temperature. The use of foraminifera and other carbonate-bearing microorganisms for clumped analysis, although perhaps more useful of paleoclimate reconstruction, is much more difficult because of restraints on sample size, thus there have been relatively few studies.

Recently there have been investigations into the differences between potential vital effects or stable isotope effects affecting the Δ_{47} system. Tang et al. (2014) showed that degassing of CO_2 from solution may effect the precipitating carbonate because the dissolution of CO_2 has distinct kinetic isotope effects. Additionally, Tripati et al. (2015) investigated the possibilities of a pH dependency on Δ_{47}. They found that Δ_{47} in fact does seemingly vary with pH, as different DIC species have distinct Δ_{47} values. This work, however, was done in context of coral calcification and was shown to mostly affect the Δ_{47}-$\delta^{18}O$ relationship. No work on vital effects or kinetic effects has been applied to planktonic foraminifera.

The analytical requirements for the clumped thermometry are much higher than other geochemical systems. Temperatures between 1 ^{o}C and 50 ^{o}C, have Δ_{47} values that vary between 0.750-500‰. Since the mass 47 isotopologue is so rare, 46 ppm of all CO_2 molecules, the analysis requires a minimum of 15 mg per sample to ensure high precision. The temperature sensitivity of the method, as described in Ghosh et al. (2006a), is defined as .004-.005‰/ ^{o}C, thus all external error needs to be minimized to ensure uncertainty of +/- 1^{o}C. The proxy may work best with large changes in SST because of the lack in range of potential Δ_{47} values, and it may not be applicable for high-resolution data over relatively small time periods (Grauel et al., 2013).

For this study, we will focus on the Zaarur et al. (2013) calibration, which provides slightly revised Δ_{47}-temperature regression, with regards to Ghosh et al. (2006a). Zaarur et al. (2013) used both synthetic and biogenic calcite, and the data presented in Ghosh et al. (2006a), to limit the calibration's error, and to expand the calculable temperature range. Foraminifera, have been shown to fit this calibration with less variance than most biogenic sources (Zaarur et al., 2013), which is discussed later in the introduction. In this study, we use the calibrations found in Zaarur et al. (2013) (below) because the synthetic carbonates used for this calibration were measured in the same laboratory, with the same protocol as our unknown samples. We also employ equations calibrated in Grauel et al., (2013), which include more foraminifera data than those in Zaarur et al. (2013), and include calibrations for the calculated $\delta^{18}O$-based temperatures.

$$\mathbf{\Delta_{47,abs} = (0.0555 \pm 0.0027)10^6/T^2 + (0.0807 \pm 0.0079)}$$

Equation 4 is adopted from Zaarur et al. (2013) Temperature is recorded in Kelvin and Δ_{47} in ‰.

$$\mathbf{\Delta_{47,ghosh} = (0.0526 \pm 0.0025) \times 10^6/T^2 + (0.0520 \pm 0.0284)}$$

Equation 5 is adopted from Zaarur et al. (2013) and represents the calibration in the Ghosh et al (2006a) reference frame. Both inorganic and biogenic carbonates are accounted for in creating this regression. Temperature is recorded in Kelvin and Δ_{47} in ‰.

$$\mathbf{\Delta_{47,ghosh} = (0.050581 \pm 0.0007)10^6/T^2 + (0.0780 \pm 0.0298)}$$

Equation 6 is sourced from Grauel et al. (2013). The calibration is founded on inorganic calcite and planktonic foraminifera observations.

1.3 The use of foraminifera in paleoclimatology

Foraminifera are single-celled, heterotrophic protists that precipitate calcite tests (via biomineralization). Fossil species are abundant for the last 540 million years, making foraminifera excellent archives of past climates due to their ubiquity throughout the more recent geologic record, and because well-preserved cores are not uncommon. Accounting for 30-80% of all carbon export in the oceans, foraminferal calcification follows the principles of carbonate mineral precipitation, although not often at equilibrium with the surrounding seawater (Lombard et al., 2010). This disequilibrium is accounted for as vital effects recorded for specific species.

We focus on planktonic foraminifera because of their potential for reconstructing sea surface temperatures (SST). Of the estimated 4,000 species of extant foraminifera, only 40

distinguishable species are planktonic, which exhibit a variety of life cycle processes and preferences. Planktonic species are visibly distinct from benthic foraminifera in that they are glossy yet textured with visible, spherical chambers, whereas benthic foraminifera lack similar texture and dimensions. Different planktonic foraminiferal species calcify uniquely depending on seasonality, temperature, and whether or not they grow with photosymbionts. There is a limited amount of divisive literature to constrain the specific depth habitats and calcification processes for specific species, but general patterns in their life cycles and lifestyles are beginning to be understood (eg; Ezard et al., 2015; Be and Hemmlin 1962; Cléroux et al., 2013).

Over the past fifty years, geochemists have used species-specific carbonate tests, both calcite and aragonite, in isotopic studies (measuring $\delta^{18}O$ and $\delta^{13}C$) to determine the growth temperature and processes of specific foraminifera. Calcification is, in many species, biologically mediated, and thus there is a high likelihood of biological fractionation. In several cases, biomineralization is orders of magnitude slower than inorganic calcite precipitation, showing clear signs of vital effects dependent on species. Moreover, foraminiferal calcification differs with ontogeny. As foraminfera age, they build successive chambers, often at different depths, with periods of rest and feeding in between chamber events. They tend to live from weeks to months, and often throughout the water column (Pearson, 2012). Issues arise with reconstructing past temperatures with bulk planktonic foraminifera because of species turnover throughout time and because of the lack of constraint on species-specific vital effects. The $\delta^{18}O_{carbonate}$ of foraminiferal tests is dependent on growth temperature, $\delta^{18}O_{seawater}$ at the site of calcification, and to small extent the carbonate ion concentration (Pearson, 2012). Because we can only assume $\delta^{18}O_{seawater}$ of the past, SST reconstructions using foraminiferal carbonate have high uncertainty, as previously discussed (Ezard et al., 2015). Additionally, many species have been found to not calcify at equilibrium, lending more uncertainty to the proxy.

In addition to $\delta^{18}O_{seawater}$, there are numerous variables involved in setting the isotopic composition of foraminifera tests**.** Ezard et al. (2015) ran a statistical analysis to determine how different variables affect the components of the fractionation temperature dependence. The study concludes that vital effects, symbionts, and maximum adult body size are fundamental in determining the species-specific temperature-$\delta^{18}O$ relationship. Despite the complications such vital effects may have on estimating temperature, isotopic studies are useful in determining depth

habitats and calcification environments for specific species, which can then be applied to calculating temperature. Using clumped isotope thermometry we hope to reduce such multivariable dependence.

1.4 Analytical Restraints on Clumped Isotope Analysis of Foraminifera

Foraminifera are difficult, yet important organisms for evaluating clumped isotopes in carbonate because of the potential for streamlined sea surface temperature reconstructions. There are recurrent differences involving the required sample size when specifically evaluating foraminifera for clumped isotopese. Foraminifera, as previously stated, are microfossils, and thus numerous specimens are required for each sample. Different studies that have sought to apply clumped carbonate analysis to foraminifera have navigated this challenge in variant ways. Because the analysis requires a large sample size, it necessitates countless hours of handpicking for a monospecific analysis or novel methods for measurement. Schmid and Bernasconi (2006) developed an automated system that measures small aliquots of carbonate (200µg), repeatedly, which reached similar analytical precision compared with studies using larger sample size. However, this work claimed to allow for a high-resolution $\delta^{13}C$ and $\delta^{18}O$ record, but a low resolution clumped analysis. Other studies handpick the required amount from large size fractions, which is extremely time intensive.

There are two studies to date that assess how foraminifera specifically fall within previously defined calibrations, both use a monospecifc analysis. Tripati et al. (2010) evaluated both foraminifera and coccolithophores using the Ghosh et al. (2006a) reference frame. The study utilized 24 samples with planktonic foraminifera, composed of four different species. Tripati et al. (2010) followed the procedures presented in Ghosh et al. (2006a), and picked foraminifera that were greater than 250µm, to exclude juveniles, with a replicate size ranging from 4-12mg. The analysis shows that all species of planktonic foraminifera tightly fit the Ghosh et al. (2006a) calibration. Their new resulting calibration can be found in Table 1.

Similarly, Grauel et al. (2013), evaluated seven species of foraminifera, five of which are planktonic, to create a new calibration (see Table 1), which includes the data in the Tripati et al. (2010) calibration. This study, however, employed the procedures created in Schmid and

Bernasconi (2010) that as previously stated, involves a smaller sample size with additional replicates on an automated aliquot-sipping system (Kiel Device). Similar to the results of Tripati et al. (2010), the authors note that foraminifera at low temperatures, namely polar species, may be suspect to kinetic isotope effects because of degassing, which is further explained in Eiler (2011) and Tang et al. (2014). This may be a result of the pH dependence of the proxy, as the clumped signal may vary with DIC composition (Tripati et al., 2015). Despite small variances in polar species, the calibration presented is seemingly robust, corresponds well with Tripati et al. (2010), and deviates only slightly from the Ghosh et al. (2006a) calibration. The calibrations resulting from these studies progressively decrease the slope of the original, inorganic calibrations.

Because most biogenic studies agree with the Zaarur et al. (2013) calibration, and because we utilized the same laboratory equipment and standards, this study evaluates the potential of bulk foraminifera for clumped isotope analysis with reference to the Zaarur et al. (2013) calibration. We also utilize the calibrations presented in Grauel et al. (2013) because they are specific to planktonic foraminifera. Most work in this area is aimed at improving instrumentation to decrease required sample size; instead we expand what consists of a valid sample. We do this by evaluating modern bulk planktonic foraminifera from three different core tops, and by evaluating different size fractions of bulk planktonic foraminifera at one specific core site dated to the mid Eocene.

2.0 Methods

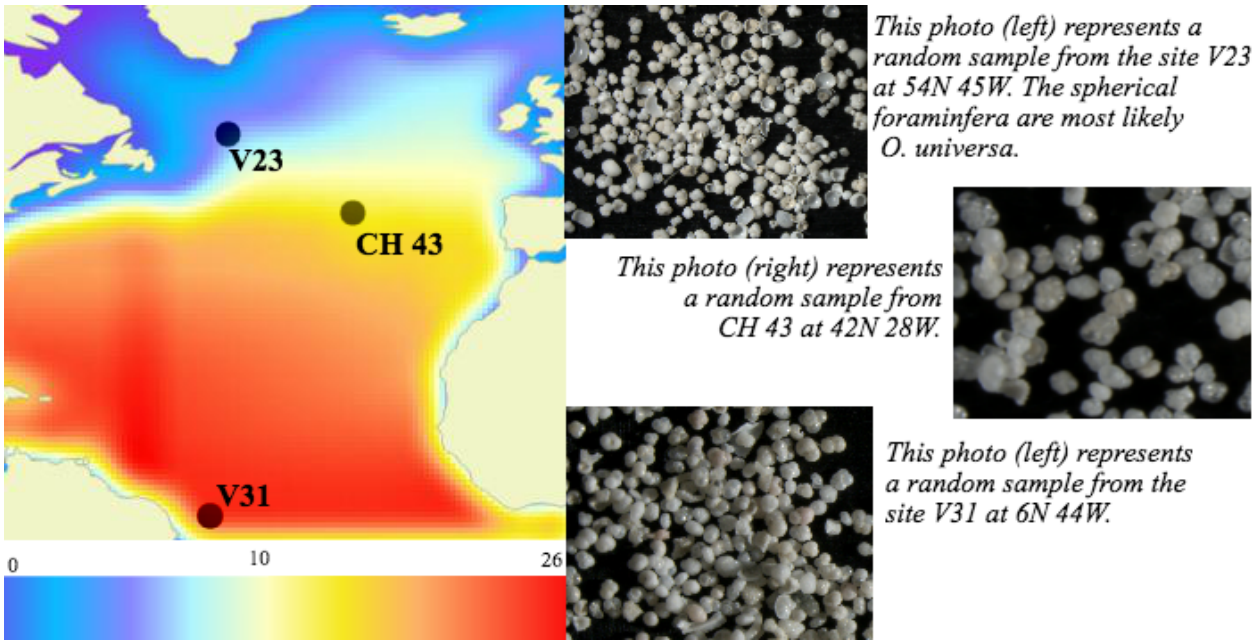

Figure 2. The above map details modern SST and core sites from which core tops were obtained. SST is reported as the mean annual temperature (MAT) sourced from the World Ocean Atlas (WOA). The corresponding photos capture the species distribution in the modern samples. In total, most of the unpicked samples consist of macroperforate planktonic foraminifera and their fragments, with less microperforate planktonic species and benthic foraminifera. Note: all the images are at varying magnifications.

2.1 Core Site Description

The modern bulk foraminifera were sourced from three core tops, belonging to the University of Rhode Island, to capture a cold signal (V23-22) ('V23') at 54 °N 45 °W, a temperate signature (CHN43-1-109-32) ('CH 43') at 42 °N 28 °W, and a warm signature (V31-134) ('V31') at 6 °N 44 °W, as seen in Figure 2.

The Eocene samples were sourced from IODP expedition 342, U1408C-19H-7, in the western North Atlantic at 41.26°N 49.47°W. Expedition analysis shows that this section has good to exceptional preservation in the Middle Eocene. The sample consists of distinguishable *O. beckmanni*, *Hantkenina spp*, and *G. nuttalli* (Norris et al., 2014).

2.2 Temperature Estimation

To estimate a corresponding temperature of the bulk foraminifera, rather than assuming mean annual temperatures (MAT) of the sourced surface waters, we investigated the biological constraints on the calcification temperature. Planktonic foraminifera may calcify seasonally or at different depths depending on the species and latitude. As specified previously, foraminifera calcification may follow algal blooms or may be linked to that of photosymbionts. Thus, in identifying temperature, we assumed overarching patterns for apparent species, founded in literature, based on the region at which each sample was collected. Total species categorization was difficult because most foraminifera at this size fraction are indeterminable as many are still juvenile and had yet to complete all of their identifiable chamber construction.

The high latitude foraminifera, as described in Schiebel and Hemleben (2005) and Chapman (2010), are highest in concentration during the summer. The estimated temperature for our high latitude site, V23-22, is the mean upper mixed layer summer temperature over the past six decades, calculated through the World Ocean Atlas (WOA). The estimated temperature is 10.8°C. The most distinguishable species within this sample is *O. universa*, which in particular grows at the surface and in response to its photosymbionts. This provides further evidence for a seasonal signal, as the photosymbiont growth is seasonal, as well as evidence for an upper mixed layer (photic zone) signal.

The temperate site, CHN43-1-109-32, was also assumed to record more of a seasonal signal. Temperate foraminifera, similar to those at high latitudes, are in highest concentrations during the spring and fall. According to Weinkauf et al. (2003), the temperate latitude species have two main peak concentrations, late spring and late summer. The symbiont baring species bloom late in the spring (April/May) following their photosymbionts, whereas the non-symbiont baring species bloom late summer (August/September). Thus, the estimated growth temperature at this site was calculated using the average of WOA mean for those specific months over the past six decades in the upper mixed layer. The estimated temperature is 18.0°C. The most common species at nearby sites (ODP expedition 957 sites 950-952) are *G. inflata, O. universa, G. Ruber, and G. Bulloides*, the latter three all occur in mixed layer, whereas *G. inflata* resides in the thermocline (Ezard et al., 2015). All of these species, however, as described in Fairbanks et

al. (1980), calcify in the upper mixed layer despite where they reside within the water column. So the surface water temperature estimate holds. For the seasonal estimate to be refined, an exact species analysis would be needed.

The tropical site, V31-134, does not follow a similar seasonality assumption. As evidenced in the literature (Farmer et al., 2007, and Schiebel and Hemleben 2005), tropical foraminifer concentrations are fairly consistent annually, but tropical species calcify at varying depths into and perhaps even below the thermocline. Their life cycles are not continuous within the surface. It was particularly hard to distinguish species for this site. Thus, using the analysis in Ezard et al. (2015), the best estimation of temperature was to account for all possible depth habitats. To estimate the most appropriate temperature for the tropical sample, we average the mean annual temperatures from the surface to the thermocline. The estimated temperature is 25.7°C. For a description of species possibilities at each site see Appendix Table 2A, which reorganizes the data presented in Ezard et al. (2015).

2.3 Sample Preparation

The modern samples were sieved at around 65-200μm, a rarely used foraminifera sample portion comprising both of juveniles and adults. The Eocene samples were sieved into the following size fractions: 60-150μm, 150-250μm, and greater than 250μm. All samples were then handpicked under a microscope to remove any benthic foraminifera, remaining sediment, or other non-foraminiferal material. Samples were photographed and compared to nearby core-tops to determine species composition.

2.4 Sample Analysis

We followed procedures outlined in Zaarur et al. (2013). All replicates for each site were weighed for at least 3.8mg and no more than 5mg. Samples were then added to the McCrea style reaction vessels, along with H_3PO_4 (ρ = 1.95 gr/cm^3). Before dissolving the carbonate material, the samples were pumped to rid the chambers of atmospheric air. Samples were reacted over night at 25°C to ensure full reaction and a consistent digestion fractionation with previous calibration studies at 25°C. The accepted fractionation factor of digestion at 25 °C in the

literature for $\delta^{18}O/\ \delta^{16}O$ is 1.01245 (Zaarur et al., 2013). CO_2 was cryogenically captured, using liquid nitrogen and organic solvents, rid of non-condensable gasses on a vacuum line, and cleaned through a Gas Chromatograph (GC) to purge the samples of organic impurities. Measurements were taken on ThermoMAT253 gas source isotope ratio mass spectrometer, modified specifically to measure 44-49 in a dual inlet mode with count time of 8 seconds (Zaarur et al., 2013).

The system was standardized using a set of CO_2 gases heated to 1000°C for two hours to guarantee a random distribution of all CO_2 isotopologues. Δ_{47} is defined as the excess of mass 47 signal as compared to that of the random distribution. The data is reported, however, in both the Ghosh et al. (2006a) 'Ghosh' and the absolute reference frames for the sake of comparison to other recent studies and future comparisons. $\delta^{18}O$ and $\delta^{13}C$ were simultaneously measured, and were recorded in Vienna Pee Dee Belemnite (VPDB) or in the case of $\delta^{18}O$ converted to the Vienna Standard Mean Ocean Water (VSMOW) scale. We used a pre-calibrated reference gas (CO_2) from Oz-tech to calculate both signatures.

2.5 Instrumental Precision

The error within the mass spectrometer is the limiting source of error. Known as shot noise error, or Poisson error, it is measured internally. The equation for determining such error is $SEp(\Delta_{47})=SE_0(\Delta_{47})/t^{1/2}$, where $SE_0(\Delta_{47})$ is the standard error of 1s of count time. Our protocol calls for 1800s of count time, and thus the internal error ($SEp(\Delta_{47})$) is reported as 0.0084‰ (Zaarur et al., 2013).

3.0 Results

3.1 Bulk Carbonate Calibration

Sample	$\Delta_{47,ghosh}$ ‰	$\Delta_{47,abs}$ ‰	$\delta^{18}O$ ‰	Estimated Temperature °C
V23	0.685	0.747	1.40	10.8
CH43	0.654	0.714	1.32	18

V31	0.638	0.731	-2.19	25.7

Table 2 (above**)** presents the collected data from all modern samples. The data shows the average Δ_{47}, in both reference frames, $\delta^{18}O_{carbonate}$ (VPDB), and the estimated temperature calculated using the World Ocean Atlas (WOA). This equation for this calculation can be found in Kim and O'neil (1997) (Equation 7).

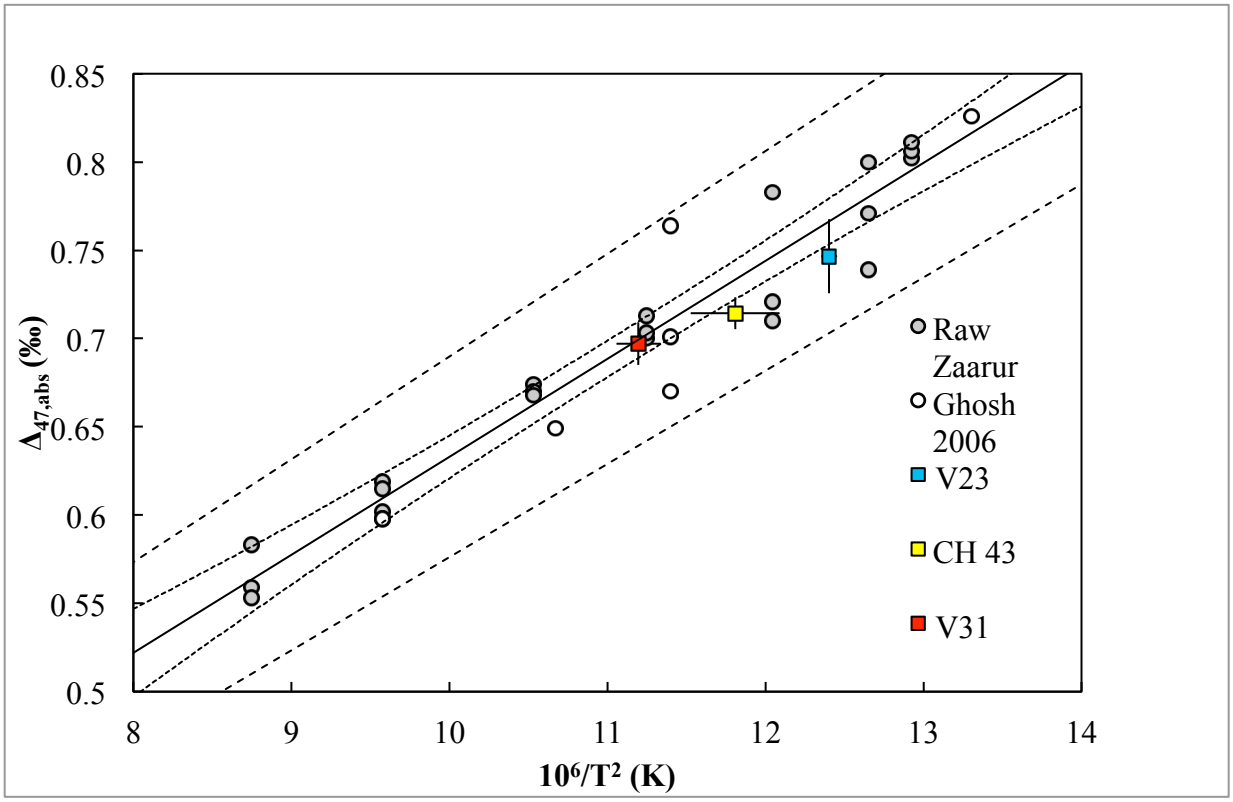

Figure 3 (above) presents the calibration calculated in Zaarur et al. (2013) populated with synthetic, raw data from both Ghosh et al. (2006a) and Zaarur et al. (2013). The values are reported in the absolute reference frame for the sake of future comparison. The figure presents the Δ_{47} data from this study (V23, CH 43 and V31). A 95% confidence interval is applied to the calibration sourced from the data presented in the previous studies. The error bars represent standard error.

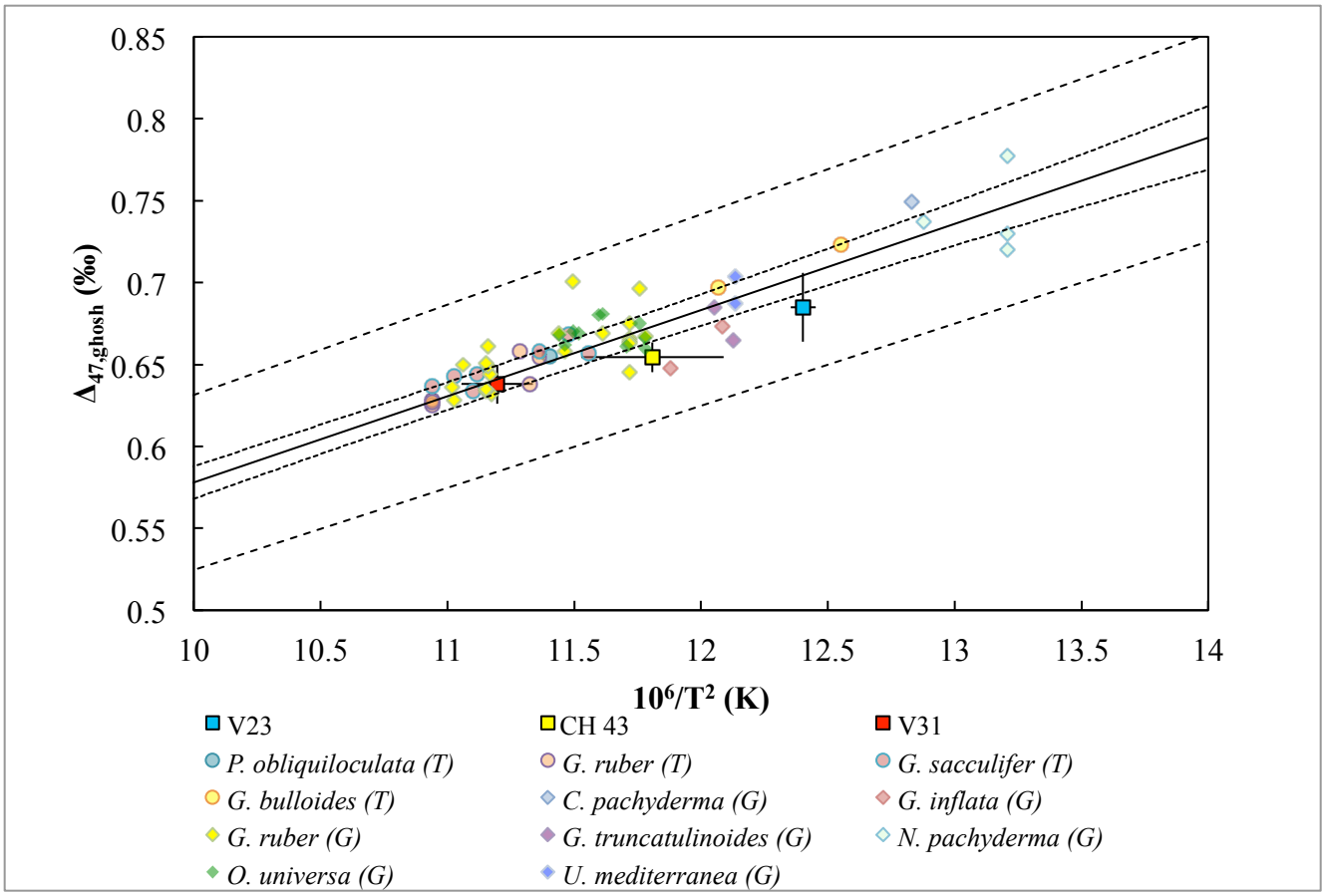

Figure 4 presents the calibration calculated in Zaarur et al. (2013) populated with raw data from both Tripati et al. (2010) and Grauel et al. (2013) alongside the Δ_{47} data from this study (V23, CH 43 and V31). All species marked with 'T' are sourced from Tripati et al. (2013), and 'G' from Grauel et al. (2013). The values are reported in the Ghosh et al. (2006a) reference frame for the ease of comparison. A 95% confidence interval is applied to the calibration sourced from the data presented in the previous studies. The error bars represent standard error.

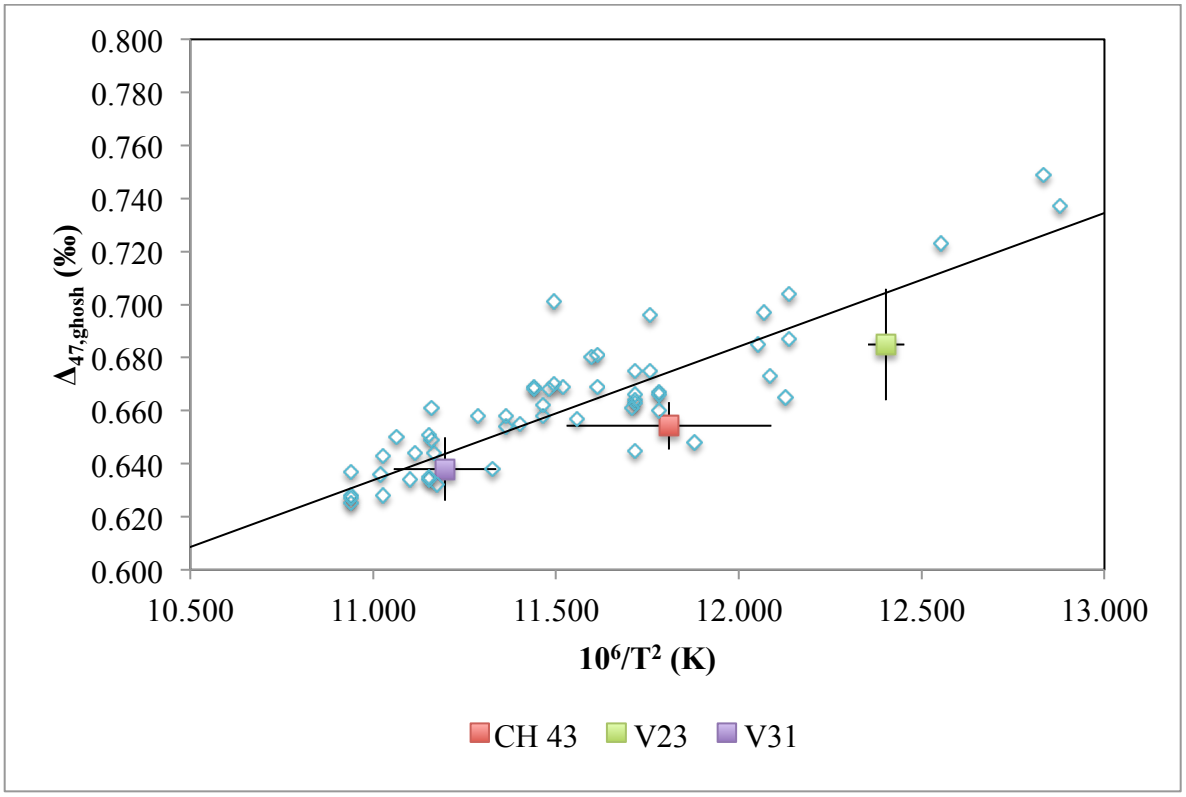

Figure 5 shows the data from this study (V23, CH 43, and V31) along Grauel et al. (2013) calibration. Temperatures represent those predicted from WOA and biological constraints. This calibration is slightly shallower than the others, and is fitted to only planktonic foraminifera data (marked in blue) and inorganic calcite data rather than including carbonate-baring macrofauna which, when included, result in a steeper slope. The error bars represent standard error.

The results indicate that the bulk foraminifera analyses for Δ_{47}, reaffirm, within reason, the calibrations determined in Zaarur et al. (2013) and Grauel et al. (2013) using the estimated atlas temperatures. The average $\Delta_{47,abs}$ values for the high latitude site, tropical site, and temperate site respectively are 0.747‰, 0.715‰, 0.731‰ with standard error being 0.021‰, 0.009‰, and 0.012‰. The estimated temperature for the tropical site falls on all of the calibration lines, whereas the other two sites show an average Δ_{47} value slightly lower than predicted. The estimated temperatures range from 10°C to 26°C (WOA).

We present the results in the absolute reference frame for comparison for future studies. The first calibration (Figure 1) uses the absolute reference frame, and the regression is based on synthetic calcite precipitation only. Almost all previous biogenic studies correspond well with this line including brachiopods, foraminifera, coccolithophores, and teeth. Figures 2 and 3 are

both presented in the Ghosh et al. (2006a) reference frame for sake of retrospective comparison. Figure 2, however, is sourced from Zaarur et al. (2013), whereas Figure 3 is sourced from Grauel et al. (2013).

We use the Kim and O'Neil (1997) regression (Equation 7) to calculate temperature from $\delta^{18}O_{carbonate}$ (VPDB) (see discussion). The average values for the high latitude, tropical, and temperate site are 1.32‰, -2.19‰, and 1.40‰ respectively with varying standard errors of 0.09‰, 0.2‰, and 0.16‰ respectively. The recorded $\delta^{18}O_{seawater}$ was 0.08‰ at the high latitude site, 0.77‰ at the temperate site, and 0.81‰ at the tropical site (LeGrande and Schmidt 2006). With Equation 7, it is possible to isolate $\delta^{18}O_{seawater}$ using the temperature conveyed by the Δ_{47} signal or the estimated temperature. Additionally, the equation is useful for reconstructing an estimated $\delta^{18}O_{carbonate}$ using the calibrated temperature from the Δ_{47} signal.

Equation 7 (below)

$$\delta 18Ocarbonate = 25.778 - 3.333\sqrt{43.704 + T(C)} + (\delta 18Osewater - .027)$$

3.2 Differing Size Fraction of Bulk Carbonates

	60-150µm	**150-250µm**	**>250µm**
Sample 1	0.701	0.671	0.698
Sample 2	0.656	NA	0.691
Sample 3	0.719	0.727	0.691
Average	0.692	0.699	0.693
Overall Average	.694		
Standard Error	.008		

Table 2 presents the collected data from the Eocene samples. The data shows the $\Delta_{47,abs}$ (‰) values per size fraction. The second sample for 150-250µm is not recorded because of a leak, leading to faulty values.

	60-150µm	**150-250µm**	**>250 µm**
Sample 1	-1.41	-1.48	-1.54
Sample 2	-1.36	-1.50	-1.46
Sample 3	-1.24	NA	-1.42
Average	-1.33	-1.49	-1.47

Overall Average	-1.43		
Standard Error	0.03		

Table 3 depicts the average $\delta^{18}O$ (‰) from the Eocene samples.

We found no statistical significance among the varying size fraction (p=0.9), using a two-tailed p-test. Thus, we can conclude that size fraction has limited effect on bulk planktonic foraminifera. The average for all replicates was 0.694‰ ±0.008‰. The results match previous proxy and modeling data that suggest that the average temperate at 41^{o}N was around 25^{o}C during the Eocene (see discussion section 4.3) (Speelman et al. 2010). The bulk samples, with clumped isotope analysis, produce an estimated temperature between 26.5-27.5^{o}C, using the calibration presented in the absolute reference frame from Zaarur et al. (2013). Assuming that the planktonic foraminifera present in the sample behave as the modern ones, this temperature would reflect the mean surface temperatures from the late spring and late summer, thus warmer than the mean annual temperature. Additionally, the $\delta^{18}O_{carbonate}$ values record a temperature of 23^{o}C assuming an ice-free world in the middle Eocene, and using Equation 7 from Kim and O'Neil (1997).

The second replicate analyzed from the 150-250μm size fraction had faulty signatures because of a leak in the vacuum system. Non-condensable gasses were recorded beyond the permissible pressure. Therefore, the sample is not recorded here. However, this shouldn't affect the conclusions because the largest ontogenetic difference should be expected between the smallest and largest size fraction. Many planktonic foraminifera have a size-dependent effect of on $\delta^{18}O_{carbonate}$ values, which is not seen here with our Δ_{47} values. The $\delta^{18}O_{carbonate}$ do differ among the different size-fractions, and may reflect the size dependent vital effects.

3.3 Standards and Accuracy

	Corn	**Heated Gas**	**YCM**
	0.871	0.017	0.321
	0.912	-0.011	0.332
	0.883	0.001	0.439
	0.871	0.002	0.340
	1.005	-0.024	0.337
	0.968	0.019	0.326
	0.842	0.019	0.476
	0.882	0.022	0.278
	0.869	0.073	0.261

	0.865	0.040	
	0.881	0.000	
	0.875		
Average	0.894	0.014	0.346
Standard Error	0.013	0.008	0.023

Table 4 shows the Δ_{47} (‰) values for all standard analyses during the sampling period. Corn is a calibrated CO_2 made to reflect $\delta^{13}C$ signatures of C4 plants. YCM is a standard marble, and heated gas is a calibrated CO_2 gas heated to 1000°C.

Throughout the duration of the sample analyses, three standards were run. The largest standard error on the samples was about 0.02‰. The long-term standard error is 0.004‰. We did not have to correct for temporal variability because the samples did not follow any trend over time, despite the overall variability. The variation in temperature, calculated from the variation in Δ_{47} is .004, reported in $10^6/T^2$ (T is in Kelvin).

4. Discussion

The motivation of this study is to identify whether bulk planktonic foraminifera, rather than species-specific methods, can be used in clumped isotope thermometry in order to reduce the sample constraints associated with monospecific analyses. We find that bulk foraminifera, as compared to previous monospecific analyses, match the calibration within error, and that size fraction may be irrelevant. This follows assumed physics of 'clumping' given that clumping is thermodynamically controlled, is set the mineral lattice during precipitation, and seems to evade vital effects. In the following section, we outline the limitations and assumptions associated with analyzing bulk foraminifera in modern core tops, and how defining these assumptions are necessary in ensuring accurate clumped isotope paleothermometry in the future.

4.1 Growth Temperature Assumptions

If accurately interpreted, like with all proxy data, clumped isotope thermometry of bulk planktonic foraminifera will provide valuable insights in reconstructing SST. Because the scale is quite small given the range of temperatures, the proxy is best used for large-scale SST changes rather than high-resolution reconstruction (Finnegan et al., 2011). It is imperative that the

interpretations are detailed and that the assumptions are comprehensive. In this study, much effort was spent in evaluating accurate temperature estimates for the modern samples.

Planktonic foraminifera are not uniform in their calcification processes. The most uncertain assumption associated with bulk foraminifera is the temperature and habitat of calcification given that each samples is composed of a variety of species. The process is highly species and region-dependent and thus hard to quantify when doing bulk analysis. Moreover, the modern samples were composed of a mix of juvenile and adult foraminifera, which presents an even more complicated scenario. Calcification processes are different for juveniles than they are for adults, as adults add additional calcite chambers at different depths (Pearson, 2012). For temperature estimations, we followed the prevailing theories of regional foraminifera growth.

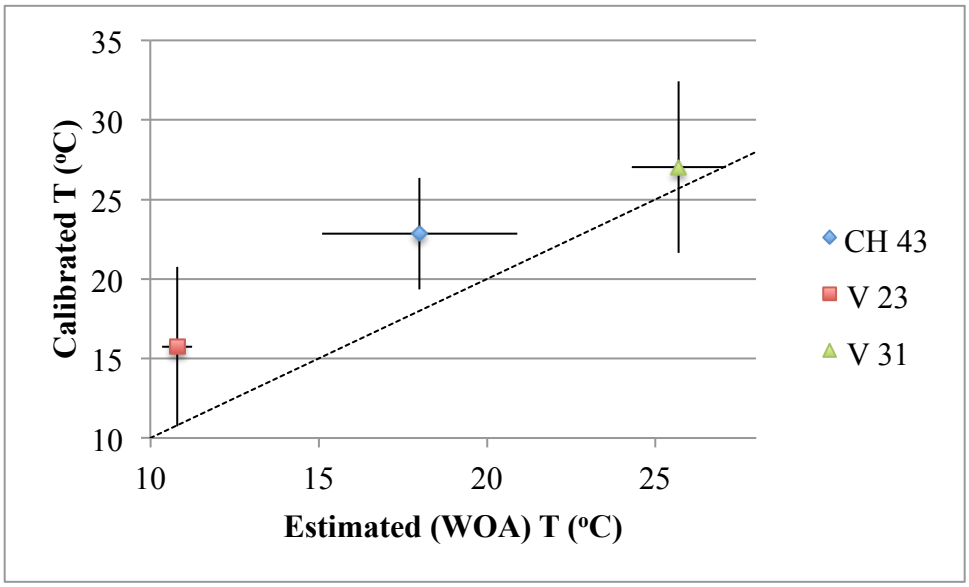

Figure 4 (above) shows the relationship between estimated temperatures and calibrated temperatures calculated from the Δ_{47} using the Zaarur et al. (2013) calibration. The estimated temperatures are those assumed based on foraminifera biology and WOA analysis. Data is compared to the line y=x. The error bars represent standard error.

The high latitude and temperate site temperature estimates were colder than the Δ_{47} calibration line predicted. The high latitude site accounted for the largest standard error among replicates. Both of the samples, however, when uncertainty is accounted for, are within the 95%

confidence interval of all calibrations. The tropical signal conveys a temperature more or less equal to what was predicted. Small discrepancies, in general, may be a result of slightly misinterpreted estimated temperatures or general precision error embodied in any part of the procedures. We can ignore isobaric error because it would result in significantly lower Δ_{47} values.

The presence of *O. Universa* in the northernmost site is an indication of potential input from the Gulf Stream. Planktonic foraminifera do move with currents, and *O. Universa* is in high concentrations within the Gulf Stream system (Bé and Hamlin 1962). Thus the signal being read at this site could be more reflective of warmer waters sourced from the Gulf Stream, given that this site sits off the coast of Newfoundland and is subject to eddies. This would account for some of the deviation from the calibration and perhaps the large standard error at this site. This is not reflected, however, by $\delta^{18}O_{carbonate}$ values (Figure 5).

The previous two studies (Tripati et al., 2013; Grauel et al., 2013) had difficulties constraining their high latitude species because of their variable life cycles and their inclusion of species that occur below the thermocline. Some species were found calcifying at different depths from where they lived or reproduced. These unknown habitat preferences may convolute our data because we evaluate young foraminifera, many of which do not have their secondary chambers that develop with age, and little is understood about their biology.

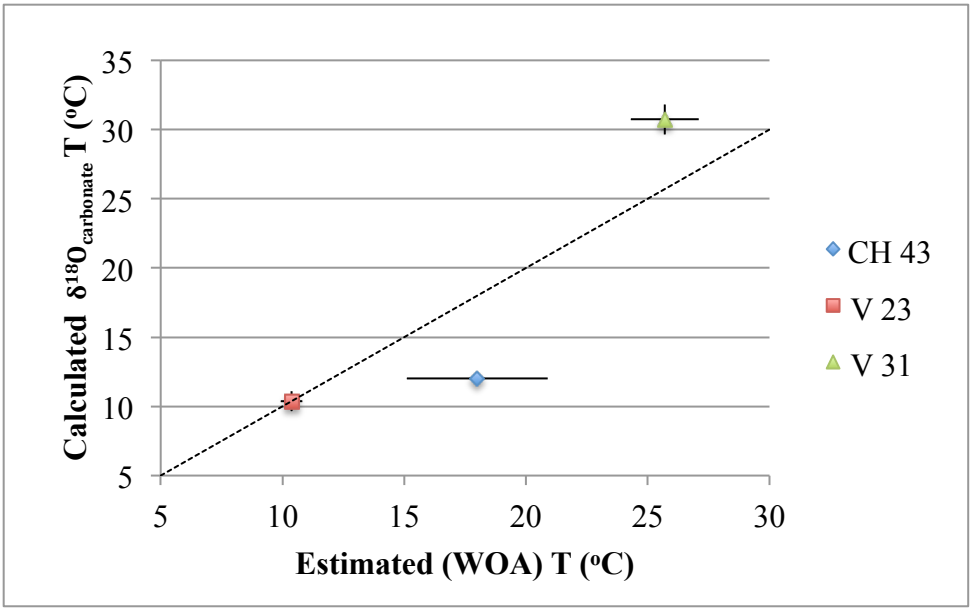

Figure 5 (above) describes the relationship between the $\delta^{18}O$-calculated calcification temperatures using the equation provided in Kim and O'Neil (1997), and the estimated calcification temperatures, as compared to line y=x. The error bars represent standard error.

The Δ_{47} signal likely represents the depth and temperature at which reproduction and early growth occurs, which are some of the least understood areas of foraminiferal biology. Planktonic foraminifera reproduction has never been successfully observed in laboratory settings (Elder, personal communication). Many studies indicate that foraminifera reproduce on a lunar cycle, and many species actively dissolve their shells for reproductive purposes (Erez et al., 1991). Juvenile foraminifera would then show an upper surface temperature rather than a more complete mixed layer signature because this lunar reproduction brings the foraminifera to the surface, and perhaps accounts partly for the warmer signal in our data. Small changes in microenvironments caused by shell dissolution and reproduction may be reflected in the Δ_{47} residual. The temperature estimates, however, correspond well, with the exception of the temperate site, with the calculated $\delta^{18}O_{carbonate}$ temperature as seen in Figure 5. Although the temperature estimates remain uncertain, they are reinforced by the $\delta^{18}O_{carbonate}$ data. This relationship, although, seemingly robust, may not hold if the foraminifera are not calcifying in equilibrium with the surrounding environment.

4.2 $\delta^{18}O$ and Temperature Analysis

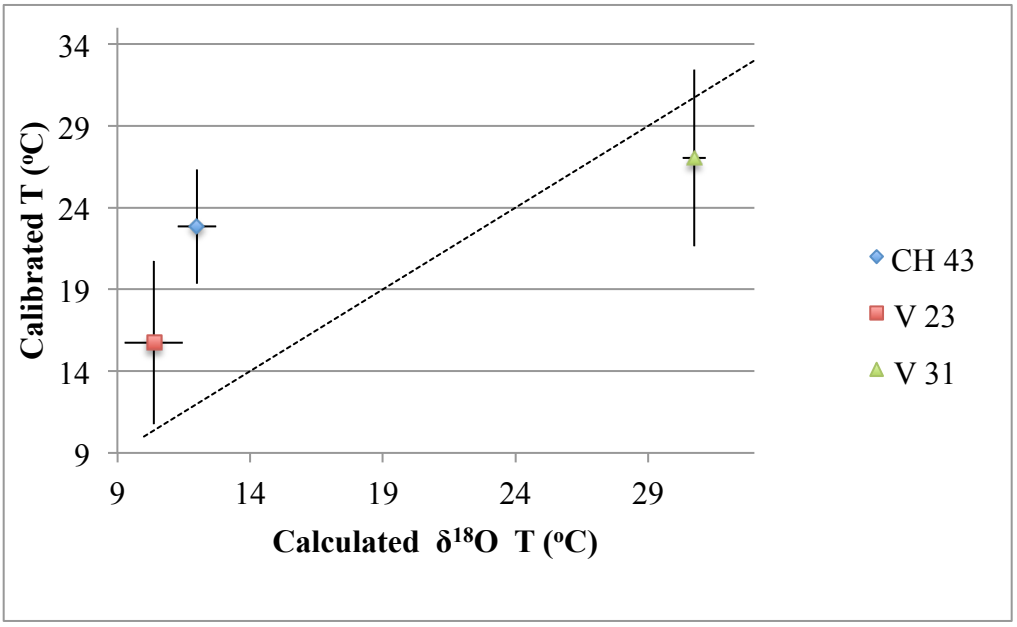

Figure 6 (above), details the relationship between the $\delta^{18}O$-calculated temperatures (Kim and O'Neil, 1997) and the calibration curve (Zaruur et al., 2013) as compared to the line y=x. The error bars represent standard error.

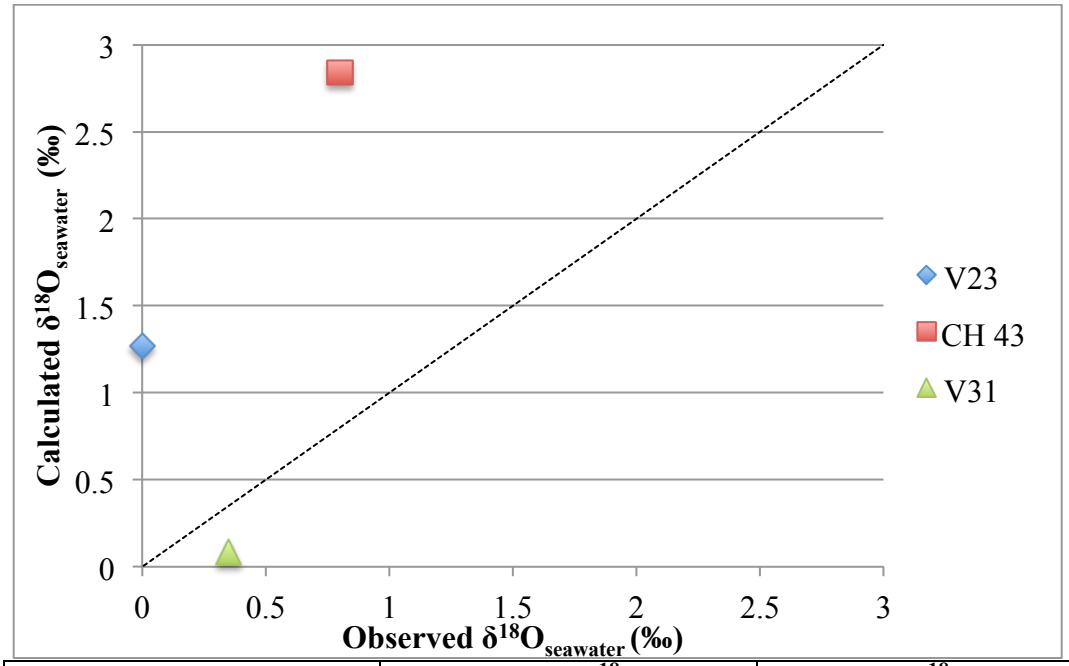

Sample	Δ_{47} predicted $\delta^{18}O_{seawater}$ (V-SMOW) (‰)	Observed $\delta^{18}O_{seawater}$ (V-SMOW) (‰)
V23	1.27	.08
CH 43	2.84	0.77
V31	0.09	0..81

Figure 7 and Table 5 portrays the observed $\delta^{18}O_{seawater}$ from LeGrande and Schmidt (2006), and the estimated $\delta^{18}O_{seawater}$, which is calculated using the Δ_{47}–calibrated temperature and the measured $\delta^{18}O_{carbonate}$ as the inputs into Kim and O'Neil (1997) equation. The data is plotted against the line y=x.

There is evidence of vital effects based on the mismatch between the observed and predicted $\delta^{18}O_{seawater}$ and $\delta^{18}O_{carbonate.}$ (Figures 7,9 and Tables 5,6). These vital effects, in addition to the error surrounding the small scale of Δ_{47} measurements, affect the $\delta^{18}O_{carbonate}$ signal, making it difficult to constrain $\delta^{18}O_{seawater}$. $\delta^{18}O$ (VPDB) values for all samples, as shown in Table 6 and Figure 7, was not in equilibrium with the seawater at each corresponding site $\delta^{18}O$ (V-SMOW) according to the Zaarur et al. (2013) calibration and the Δ_{47} signal. The $\delta^{18}O$ (VPDB) of the samples may describe calcification temperatures at that site assuming constant salinity, DIC, and equilibrium. Because of the disequilibrium, we can assume that the $\delta^{18}O_{seawater}$ calculated using the Δ_{47} signal and the $\delta^{18}O_{carbonate}$ is representative of both temperature and the microenvironment created through the biogenic calcification process. For example, some species transport seawater into their vacuoles in which the calcite test is precipitated and transported

(Pearson, 2012). As described in the literature, $\delta^{18}O_{carbonate}$ reflects clear effects of symbioses for size-specific tests, and significant species-dependent effects (Ezard et al., 2015). We see such size-dependent effects within our own study. The Eocene samples show different $\delta^{18}O_{carbonate}$ between the smallest and largest size fractions. Without knowing the specific species comprising the modern samples, and their relative concentrations, it is hard to discern how much of the $\delta^{18}O_{carbonate}$ signal is the result of vital effects.

Despite showing disequilibrium, the assumed calcification temperatures from the oxygen signatures shows no specific trend with regards to the estimated temperature, and overall, correlate relatively well (Figure 5). At the temperate site, however, $\delta^{18}O_{carbonate}$ values convey a significantly colder than estimated temperature. At this site, calcification is seasonal and dependent on species (Weinkauf et al., 2003). Perhaps, the values could be recording the late spring peak in foraminifera concentration associated with photosymbiont-baring species. Unfortunately, species composition is hard to determine in this study due to the size limitations of the small size fractions. The oxygen signatures, since they are recording a much colder temperature, specifically at the temperate sight, than Δ_{47}, do not have as robust of a relationship with the calibrated (Δ_{47}) temperature as the estimated temperatures. The tropical site is the exception, where the $\delta^{18}O_{carbonate}$ provides slightly warmer temperature, but relatively consistent with the mean annual temperature of the upper mixed layer (Figure 6). It may be likely then, at the tropical site, that the mean summer temperature of the entire mixed layer slightly underestimates the calcifying temperature. If the foraminifera are mostly reproducing and juveniles are calcifying at the surface, this warmer estimation would be expected. At all sites, if the foraminifera reproduce at warmer latitudes, which would occur if surface currents are transporting foraminifera from those regions, there is potential for warm bias. This is not seen in the $\delta^{18}O_{carbonate}$ values, but these values are not at equilibrium with seawater, hence do not the most robust method for checking assumptions. Additionally, the calibration generally works less well with cold temperatures and is known to match best with samples from warmer sites, as portrayed by our data (Tripati et al., 2015).

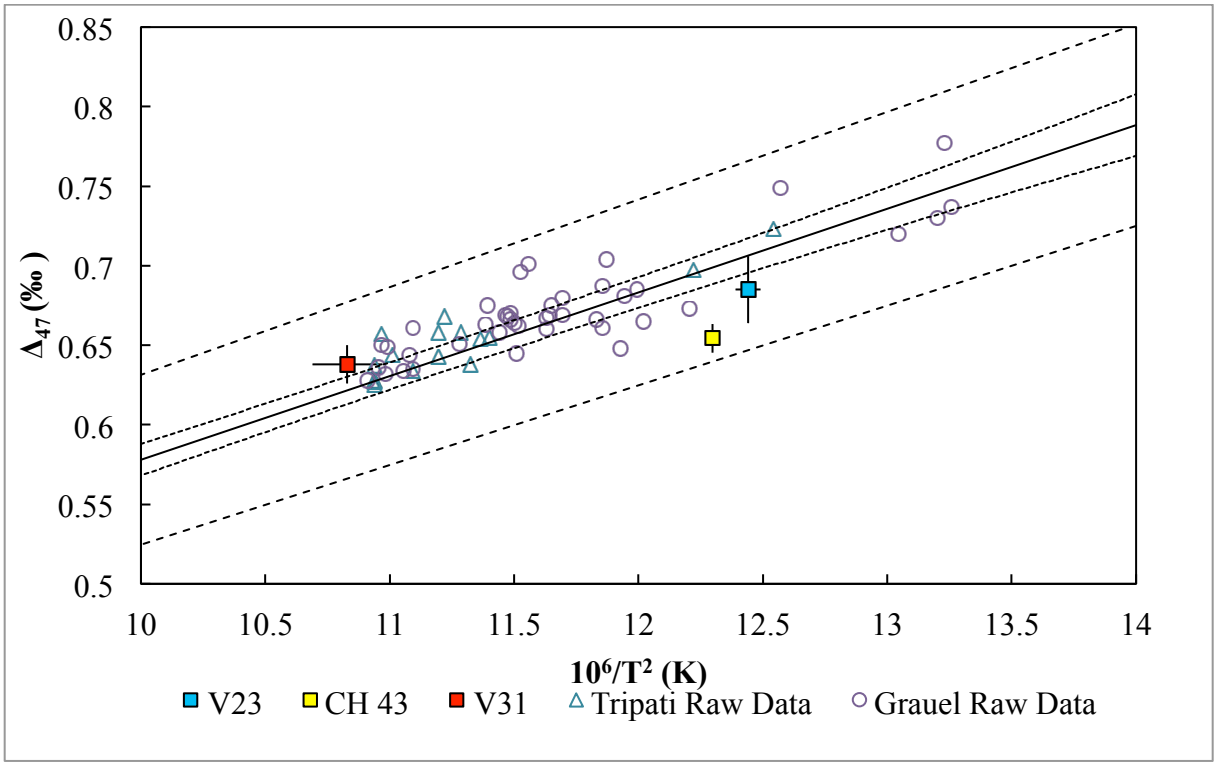

Figure 8 depicts the relationship between the calculated temperatures from the $\delta^{18}O_{carbonate}$ values and $\Delta_{47,ghosh}$ values , populated with raw data from Tripati et al. (2010), Grauel et al. (2013), and data from this study (V23, CH 43, and V31). Temperatures were calculated using the Kim and O'Neil (1997) equation. Observed $\delta^{18}O_{seawater}$ is sourced from LeGrande and Schmidt (2006). A 95% confidence interval is applied. The error bars represent standard error.

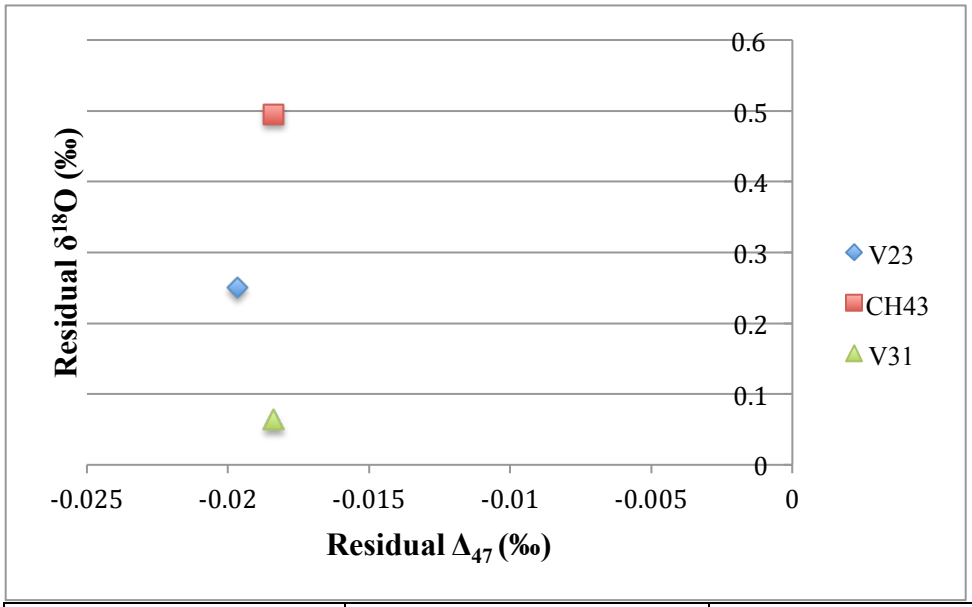

Sample	Residual Δ_{47} (‰)	Residual $\delta^{18}O_{carbonate}$ (VPDB) (‰)
V23	-0.020	0.25
CH43	-0.018	0.50

V31	-0.002	0.06

Figure 9 and Table 6 (above) The data shows the residual $\Delta_{47,ghosh}$, expected (Zaarur et al., 2013) subtracted from measured, and the residual $\delta^{18}O$, which is analyzed as the $\delta^{18}O_{carbonate}$ of inorganic calcite. To calculate these values, we entered the Δ_{47}–based temperatures and the observed $\delta^{18}O$ of seawater (LeGrande and Schmidt, 2006) as the input into the Kim and O'Neil (1997) equation, subtracted from the observed $\delta^{18}O_{carbonate}$. All $\delta^{18}O$ are recorded in VPDB.

The Δ_{47} values convey temperature within error, but may not be precise enough for predicting $\delta^{18}O$. The residual Δ_{47} is seemingly insignificant and within error of presented calibrations and within the error of our standards (Table 4) as seen in Figure 9. As stated previously, the scale .500-.750‰ is applicable for ocean temperatures, thus a small amount of error, encompassed by both instrumental precision and general uncertainty, can dramatically change interpretations of the data. The other studies were able to confine $\delta^{18}O_{carbonate}$ estimates to be within 0.1-0.3‰, which is not the case for the bulk analyses. Therefore, for the existing data, it would be recommended not to predict past $\delta^{18}O$ of seawater or carbonates using bulk planktonic foraminifera (Figures 7 and 9). Conversely, despite disequilibrium, the calculated temperatures, with the exception of the temperate site, which still falls within possible error of the slope, fits the calibration presented in Zaarur et al. (2013) for Δ_{47}- $\delta^{18}O$ temperature (Figure 8), and follow similar patterns as the estimated temperatures. The tropical site matches the calibration whereas the other sites fall below the calibration. This may be symptomatic of a broader correlation between $\delta^{18}O$, temperature, and Δ_{47}, which could result in an even shallower slope in the temperature calibration.

To more rigorously determine the temperatures at the sites, and better confine the magnitude of the vital effects, future work should incorporate organic proxies, such as TEX_{86}. Although the temperature estimates did fall well within error of the calibration line, as did the temperature reconstructions, it would be beneficial to understand exactly where in the surface ocean bulk planktonic foraminifera, are one average, setting the isotopic composition of their tests. If there is other proxy data available then we can begin to constrain the Δ_{47} signal. Seasonality and depth, two large variables in determining the clumped bulk signal, are necessary parameters for interpreting past climate when using bulk clumped planktonic foraminifera. Moreover, clumped isotope analysis may not succeed in predicting the $\delta^{18}O$ of seawater of the

past because it reflects the $\delta^{18}O$ of microenvironment in which the foraminifera calcified rather than the seawater. It does convey, however, reasonable temperature predictions.

4.3 Future work on Modern Bulk Foraminifera

The prevailing pattern of warmer Δ_{47} values for the high latitude sites, in using both temperature estimates as well as temperatures from $\delta^{18}O_{carbonate}$ may present a new, shallower calibration for bulk planktonic foraminifera. Both studies on modern foraminifera suggest progressively shallower slopes, especially for the temperatures calculated from $\delta^{18}O_{carbonate}$. Here, we do not present enough data to conclusively calibrate a new regression. However, viewing this work as preliminary, there is now an impetus to look further into this potential use of bulk planktonic foraminifera. When analyzing all data on modern planktonic foraminifera, a revised calibration is $\Delta_{47} = .0487(10^6/T^2) + .1004$, $R^2 = .8028$. This continues the trend of shallower calibrations for foraminfera, and biogenic carbonate sources in general. Though, to reiterate, such a calibration is preliminary, and more samples from bulk analyses are needed before any conclusions can be drawn. For now, any paleoclimate reconstruction using Δ_{47} of bulk foraminifera should acknowledge that the data thus far shows slightly warmer temperatures, especially for the colder sites. Regardless, in applying this proxy to paleoclimate controversies, the bulk method should be robust enough to account for a zonal gradients such as determining the validity Pliocene permanent El Niño or understanding tropical to polar gradients of past climatic changes. The method may not be best used to determine $\delta^{18}O_{seawater}$ because of this slightly warm temperature bias, although a few studies have already engaged in such work (Finnegan et al., 2011).

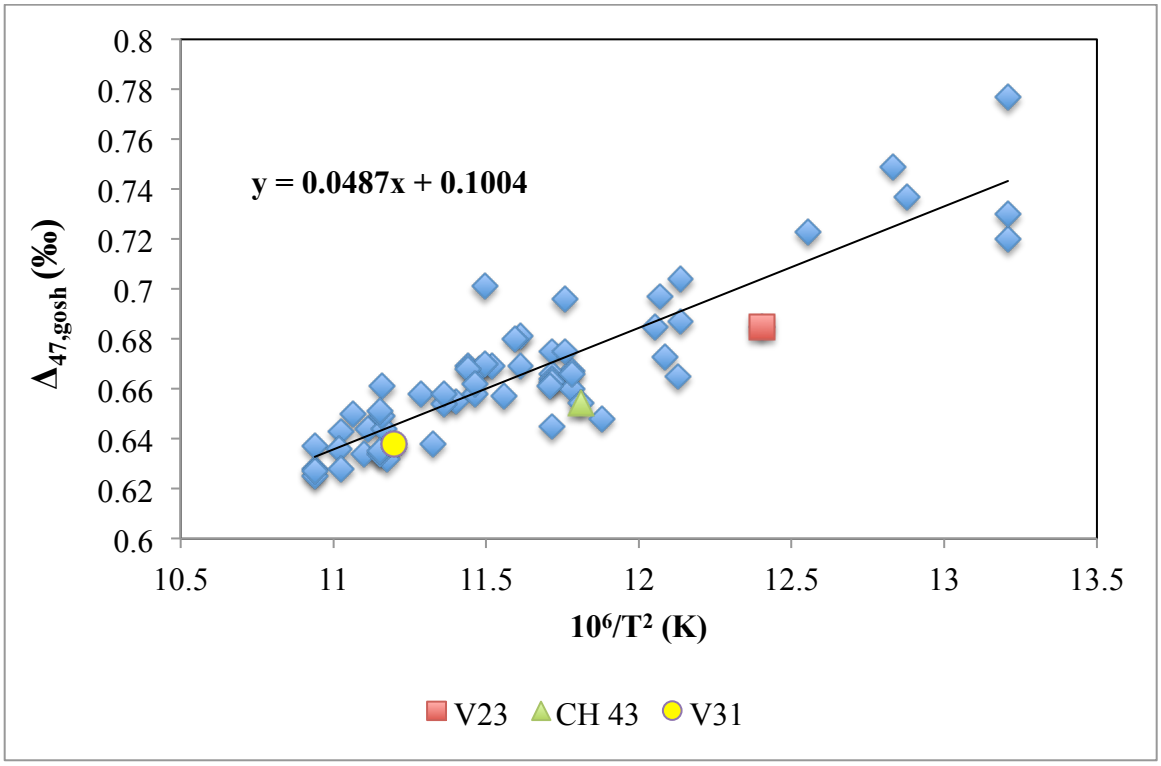

Figure 10 depicts a simple regression on all published planktonic foraminifera data including this study (V23, CH 43, V31). The equation calculated is $\Delta_{47,ghosh}=0.0487\times10^6/T^2+0.1004$.

The equation noted in Figure 10, although preliminary is remarkably similar to the most recent calibration published that accounts for potential stable isotope effects of degassing and DIC speciation (pH). Tripati et al. (2015), reports the following equation:

$$\Delta_{47,ghosh} =(0.0460\pm0.0034)\times10^6/T^2+(0.1649\pm0.0786)$$

This equation has minimal statistical difference between the calibrations presented in Figure 10. This equation was not applied to the earlier data because it was determined by inorganic calcite and coral observations, without the inclusion of planktonic foraminifera data.

We recommend additional core top analyses from additional sites with varying size fractions. Larger size fractions are especially necessary so species composition is clearer, and better constraints on the temperature estimations are possible. Moreover, three data points, although strongly encouraging, are not enough to determine conclusively whether is bulk planktonic foraminifera are a viable option for clumped carbonate isotope analyses. Furthermore, supplementary work should be done with the existing samples to reduce standard error on both the Δ_{47} values and the temperature estimates.

4.3 Eocene Sample Analysis

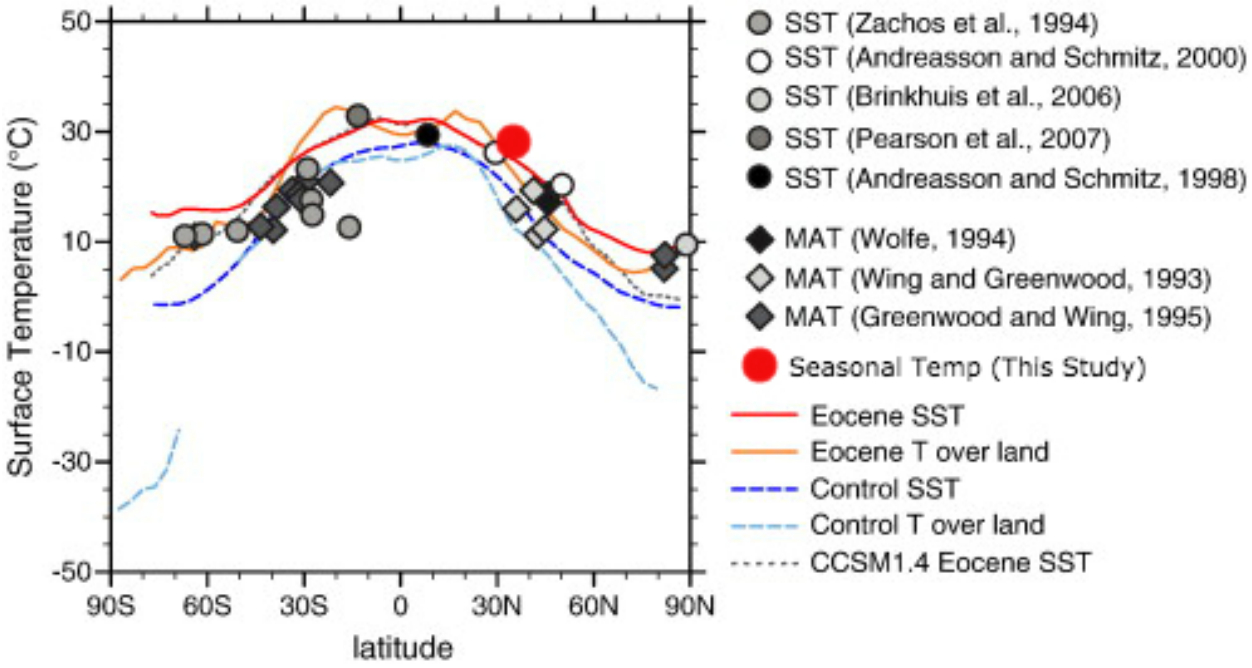

Figure 11 (adopted from Speelman et al. 2010) depicts the average temperature from the Middle Eocene samples from ODP 342-U1408-19H-7, as compared to the modeled data presented in Speelman et al. (2010). The data point, marked by the red dot, is representative of all size fractions from the site since there is no statistical difference among the varying samples. The graph is reflective of both modeling and proxy analyses.

The Middle Eocene was one of the warmest periods in the Cenozoic, thought to have little to none terrestrial ice. Benthic foraminifera record temperatures in the deep ocean 10°C warmer than modern. Equator-pole temperature gradients were reduced as expected with such warming (Speelman et al., 2010). Modeled data (Figure 11), predicts at 41°N, which is the latitude at our studied site, an SST around 25°C. As discussed in the results, the Eocene bulk planktonic samples show no statistically significant difference between the different size fractions, and record a seasonal temperature of 27°C (Figure 8). The $\delta^{18}O_{carbonate}$ values conveys a temperature of 23°C, which according to Speelman et al. (2010), is slightly cooler than expected. However, we cannot be quick to draw conclusions. Other proxy data from this site are necessary to ensure that the samples reaffirm the calibration. Thus we do not include the Eocene data in our calibration comparisons.

It is slightly surprising that the size fraction has no effect on the temperature record since larger foraminifera are known to calcify at a variety of different depths throughout their lifecycle, and that Ezard et al. 2015 shows that size has varying effects on species $\delta^{18}O_{carbonates}$ depending on their life styles. $\delta^{18}O_{carbonate}$ in this study does decrease with size, which resembles modern species that exhibit symbiosis with dinoflagellates (Ezard et al., 2015). We can assume, however, that the bulk data represents some weighted mean based of species abundance, with no influence from vital effects, and that variations in depths of calcification are not significant enough variable to shift the mean, even in the largest size fraction. It is in the largest size fraction that one would expect the greatest ontological differences in recorded temperature. This size fraction had the least standard error of the three. Within the smaller size fractions, there were a mix of juveniles and adults. Therefore, there must be some specimens in the small size fraction with more advanced chamber building that could potentially record different Δ_{47} values than the juveniles within the same sample, which have yet to build all their chambers. Whereas in the larger size fractions, consisting of more adult foraminifera, the specimens may have all completed their chamber building, and thus there is less discrepancy among the individual specimens. For further research, we would recommend comparing the error between juvenile and adult size fractions, since some of our smaller sized samples portrayed relatively large error. Overall, these results are extremely promising for foraminifera with regards to SST reconstruction because unlike $\delta^{18}O_{carbonate}$, Δ_{47} does not vary with size.. Clumped thermometry of bulk planktonic foraminifera provides a quicker, yet accurate, alternative to evaluating $\delta^{18}O_{carbonate}$ and species-specific Δ_{47}, without error due to size fraction.

5. Summary

Carbonate clumped isotope paleothermometry is limited by the size, procedures, and precision of the measurements. This is especially the case when dealing with carbonate secreting microorganisms like foraminifera. Previous studies invented new procedures and analytical techniques to navigate this challenge. Because of the need of cross-laboratory collaboration and standardization, we suggest a more standard method for avoiding the large sample size requirements of the proxy. By evaluating bulk planktonic foraminifera, we reduced the amount of picking time required for monospecific studies, especially with regards to small size fractions.

It may be impossible to run analyses of foraminifera less than 150μm in size without bulk analyses because of the picking and sample size constraints.

We conclude that our bulk analysis method is potentially just as robust as most monospecifc approaches, albeit giving slightly lower than expected Δ_{47} values compared to some single species analysis studies. When dealing with small size fractions of planktonic foraminifera, bulk analyses will save countless hours of picking. Moreover, we observed limited differences among different size fractions, suggesting that bulk analysis is useful beyond the small size fraction and among different size fractions.

More analyses bulk foraminifera need to be performed before conclusive statements can be drawn. The analyses should include additional core tops especially at higher latitudes where monospecific methods have failed. Moreover, species composition of those core tops should be evaluated in order to gain more robust assumptions regarding the average temperature of the bulk foraminifera.

6. Acknowledgements

I would like to thank my advisor Mark Pagani, for being the source of my interest in this subject, after taking classes with him every year for the past four years, and making this project possible. I would also like to thank Pincelli Hull, for allowing me to use her laboratory equipment and advising me on foraminifera biology. This work would not have been possible without Robin Canavan, who ran the vacuum lines and was there with me every step of the way. Her wisdom, especially on navigating academia, and her complete dedication to her work, and geochemistry–at-large, inspire me. Also, I greatly appreciate the time and help Leanne Elder dedicated to this project, teaching me how to physically handle foraminifera and checking over my picked samples. Thank you, Jenny Allen, who helped me compile a computer program to run the NASA and NOAA data.

8. References

Affek, H.P., and Eiler, J.M., 2006, Abundance of mass 47 CO2 in urban air, car exhaust, and human breath: Geochimica et Cosmochimica Acta, v. 70, no. 1, p. 1–12, doi: 10.1016/j.gca.2005.08.021.

Affek, H.P., Bar-Matthews, M., Ayalon, A., Matthews, A., and Eiler, J.M., 2008, Glacial/interglacial temperature variations in Soreq cave speleothems as recorded by ‘clumped isotope’ thermometry: Geochimica et Cosmochimica Acta, v. 72, no. 22, p.

5351–5360, doi: 10.1016/j.gca.2008.06.031.
Aldridge, D., Beer, C.J., and Purdie, D.A., 2011, Calcification in the planktonic foraminifera *Globigerina bulloides* linked to phosphate concentrations in surface waters of the North Atlantic Ocean: Biogeosciences Discussions Biogeosciences Discuss., v. 8, no. 4, p. 6447–6472, doi: 10.5194/bgd-8-6447-2011.
Cléroux, C., Demenocal, P., Arbuszewski, J., and Linsley, B., 2013, Reconstructing the upper water column thermal structure in the Atlantic Ocean: Paleoceanography, v. 28, no. 3, p. 503–516, doi: 10.1002/palo.20050.
Csank, A.Z., Tripati, A.K., Patterson, W.P., Eagle, R.A., Rybczynski, N., Ballantyne, A.P., and Eiler, J.M., 2011, Estimates of Arctic land surface temperatures during the early Pliocene from two novel proxies: Earth and Planetary Science Letters, v. 304, no. 3-4, p. 291–299, doi: 10.1016/j.epsl.2011.02.030.
Dennis, K.J., and Schrag, D.P., 2010, Clumped isotope thermometry of carbonatites as an indicator of diagenetic alteration: Geochimica et Cosmochimica Acta, v. 74, no. 14, p. 4110–4122, doi: 10.1016/j.gca.2010.04.005.
Dennis, K.J., Affek, H.P., Passey, B.H., Schrag, D.P., and Eiler, J.M., 2011, Defining an absolute reference frame for 'clumped' isotope studies of CO2: Geochimica et Cosmochimica Acta, v. 75, no. 22, p. 7117–7131, doi: 10.1016/j.gca.2011.09.025.
Eagle, R.A., Schauble, E.A., Tripati, A.K., Tutken, T., Hulbert, R.C., and Eiler, J.M., 2010, Body temperatures of modern and extinct vertebrates from 13C-18O bond abundances in bioapatite: Proceedings of the National Academy of Sciences, v. 107, no. 23, p. 10377–10382, doi: 10.1073/pnas.0911115107.
Eagle, R.A., Eiler, J.M., Tripati, A.K., Ries, J.B., Freitas, P.S., Hiebenthal, C., Wanamaker, A.D., Taviani, M., Elliot, M., Marenssi, S., Nakamura, K., Ramirez, P., and Roy, K., 2013, The influence of temperature and seawater carbonate saturation state on 13C–18O bond ordering in bivalve mollusks: Biogeosciences, v. 10, no. 7, p. 4591–4606, doi: 10.5194/bg-10-4591-2013.
Eiler, J.M., 2007, "Clumped-isotope" geochemistry—The study of naturally-occurring, multiply-substituted isotopologues: Earth and Planetary Science Letters, v. 262, no. 3-4, p. 309–327, doi: 10.1016/j.epsl.2007.08.020.
Eiler, J.M., 2011, Paleoclimate reconstruction using carbonate clumped isotope thermometry: Quaternary Science Reviews, v. 30, no. 25-26, p. 3575–3588, doi: 10.1016/j.quascirev.2011.09.001.
Erez, J., Almogi-Labin, A., and Avraham, S., 1991, On the Life History of Planktonic Foraminifera: Lunar Reproduction Cycle in Globigerinoides Sacculifer (Brady): Paleoceanography, v. 6, no. 3, p. 295–306, doi: 10.1029/90pa02731.
Ezard, T.H.G., Edgar, K.M., and Hull, P.M., 2015, Environmental and biological controls on size-specific δ 13 C and δ 18 O in recent planktonic foraminifera: Paleoceanography, v. 30, no. 3, p. 151–173, doi: 10.1002/2014pa002735.
Farmer, E.C., Kaplan, A., Menocal, P.B.D., and Lynch-Stieglitz, J., 2007, Corroborating ecological depth preferences of planktonic foraminifera in the tropical Atlantic with the stable oxygen isotope ratios of core top specimens: Paleoceanography, v. 22, no. 3, doi: 10.1029/2006pa001361.
Finnegan, S., Bergmann, K., Eiler, J.M., Jones, D.S., Fike, D.A., Eisenman, I., Hughes, N.C., Tripati, A.K., and Fischer, W.W., 2011, The Magnitude and Duration of Late

Ordovician-Early Silurian Glaciation: Science, v. 331, no. 6019, p. 903–906, doi: 10.1126/science.1200803.
Ghosh, P., Adkins, J., Affek, H., Balta, B., Guo, W., Schauble, E.A., Schrag, D., and Eiler, J.M., 2006, 13C–18O bonds in carbonate minerals: A new kind of paleothermometer: Geochimica et Cosmochimica Acta, v. 70, no. 6, p. 1439–1456, doi: 10.1016/j.gca.2005.11.014.
Ghosh, P., 2006, Rapid Uplift of the Altiplano Revealed Through 13C-18O Bonds in Paleosol Carbonates: Science, v. 311, no. 5760, p. 511–515, doi: 10.1126/science.1119365.
Ghosh, P., Eiler, J., Campana, S.E., and Feeney, R.F., 2007, Calibration of the carbonate 'clumped isotope' paleothermometer for otoliths: Geochimica et Cosmochimica Acta, v. 71, no. 11, p. 2736–2744, doi: 10.1016/j.gca.2007.03.015.
Grauel, A.-L., Schmid, T.W., Hu, B., Bergami, C., Capotondi, L., Zhou, L., and Bernasconi, S.M., 2013, Calibration and application of the 'clumped isotope' thermometer to foraminifera for high-resolution climate reconstructions: Geochimica et Cosmochimica Acta, v. 108, p. 125–140, doi: 10.1016/j.gca.2012.12.049.
Guo, W., Mosenfelder, J.L., Goddard, W.A., and Eiler, J.M., 2009, Isotopic fractionations associated with phosphoric acid digestion of carbonate minerals: Insights from first-principles theoretical modeling and clumped isotope measurements: Geochimica et Cosmochimica Acta, v. 73, no. 24, p. 7203–7225, doi: 10.1016/j.gca.2009.05.071.
Henkes, G.A., Passey, B.H., Wanamaker, A.D., Grossman, E.L., Ambrose, W.G., and Carroll, M.L., 2013, Carbonate clumped isotope compositions of modern marine mollusk and brachiopod shells: Geochimica et Cosmochimica Acta, v. 106, p. 307–325, doi: 10.1016/j.gca.2012.12.020.
Huntington, K.W., Eiler, J.M., Affek, H.P., Guo, W., Bonifacie, M., Yeung, L.Y., Thiagarajan, N., Passey, B., Tripati, A., Daëron, M., and Came, R., 2009, Methods and limitations of 'clumped' CO 2 isotope (Δ 47) analysis by gas-source isotope ratio mass spectrometry: Journal of Mass Spectrometry J. Mass Spectrom., v. 44, no. 9, p. 1318–1329, doi: 10.1002/jms.1614.
Kim, S.-T. and O'Neil, J. R.: Equilibrium and nonequilibrium oxygen isotope effects in synthetic carbonates Geochim. Cosmochim. Ac., 61, 3461–3475, 1997
Kimball, J., Tripati, R.E., and Dunbar, R., 2015, Carbonate "clumped" isotope signatures in aragonitic scleractinian and calcitic gorgonian deep-sea corals: Biogeosciences Discussions Biogeosciences Discuss., v. 12, no. 23, p. 19115–19165, doi: 10.5194/bgd-12-19115-2015.
Kluge, T., and Affek, H.P., 2012, Quantifying kinetic fractionation in Bunker Cave speleothems using Δ47: Quaternary Science Reviews, v. 49, p. 82–94, doi: 10.1016/j.quascirev.2012.06.013.
Kluge, T., John, C.M., Jourdan, A.-L., Davis, S., and Crawshaw, J., 2015, Laboratory calibration of the calcium carbonate clumped isotope thermometer in the 25–250°C temperature range: Geochimica et Cosmochimica Acta, v. 157, p. 213–227, doi: 10.1016/j.gca.2015.02.028.
LeGrande, A.N., and G.A. Schmidt 2006. Global gridded data set of the oxygen isotopic composition in seawater. *Geophys. Res. Lett.* **33**, L12604, doi:10.1029/2006GL026011.
Lombard, F., Rocha, R.E.D., Bijma, J., and Gattuso, J.-P., 2010, Effect of carbonate ion concentration and irradiance on calcification in planktonic foraminifera: Biogeosciences, v. 7, no. 1, p. 247–255, doi: 10.5194/bg-7-247-2010.

Pearson, P. OXYGEN ISOTOPES IN FORAMINIFERA: OVERVIEW AND HISTORICAL REVIEW, in Reconstructing Earth's Deep-Time Climate—The State of the Art in 2012, Paleontological Society, p. 1–38.

Petersen, S.V., and Schrag, D.P., 2015, Antarctic ice growth before and after the Eocene-Oligocene transition: New estimates from clumped isotope paleothermometry: Paleoceanography, v. 30, no. 10, p. 1305–1317, doi: 10.1002/2014pa002769.

Quade, J., Eiler, J., Daëron, M., and Achyuthan, H., 2013, The clumped isotope geothermometer in soil and paleosol carbonate: Geochimica et Cosmochimica Acta, v. 105, p. 92–107, doi: 10.1016/j.gca.2012.11.031.

Saenger, C., Affek, H.P., Felis, T., Thiagarajan, N., Lough, J.M., and Holcomb, M., 2012, Carbonate clumped isotope variability in shallow water corals: Temperature dependence and growth-related vital effects: Geochimica et Cosmochimica Acta, v. 99, p. 224–242, doi: 10.1016/j.gca.2012.09.035.

Schauble, E.A., Ghosh, P., and Eiler, J.M., 2006, Preferential formation of 13C–18O bonds in carbonate minerals, estimated using first-principles lattice dynamics: Geochimica et Cosmochimica Acta, v. 70, no. 10, p. 2510–2529, doi: 10.1016/j.gca.2006.02.011.

Speelman, E.N., Sewall, J.O., Noone, D., Huber, M., Heydt, A.V.D., Damsté, J.S., and Reichart, G.-J., 2010, Modeling the influence of a reduced equator-to-pole sea surface temperature gradient on the distribution of water isotopes in the Early/Middle Eocene: Earth and Planetary Science Letters, v. 298, no. 1-2, p. 57–65, doi: 10.1016/j.epsl.2010.07.026.

Norris, R.D., Wilson, P.A., Blum, P., and the Expedition 342 Scientists, 2014. Proceedings of the Integrated Ocean Drilling Program, Volume 342. doi:10.2204/iodp.proc.342.109.2014

Tang, J., Dietzel, M., Fernandez, A., Tripati, A.K., and Rosenheim, B.E., 2014, Evaluation of kinetic effects on clumped isotope fractionation (Δ47) during inorganic calcite precipitation: Geochimica et Cosmochimica Acta, v. 134, p. 120–136, doi: 10.1016/j.gca.2014.03.005.

Tang, J., Dietzel, M., Fernandez, A., Tripati, A.K., and Rosenheim, B.E., 2014, Evaluation of kinetic effects on clumped isotope fractionation (Δ47) during inorganic calcite precipitation: Geochimica et Cosmochimica Acta, v. 134, p. 120–136, doi: 10.1016/j.gca.2014.03.005.

Thiagarajan, N., Adkins, J., and Eiler, J., 2011, Carbonate clumped isotope thermometry of deep-sea corals and implications for vital effects: Geochimica et Cosmochimica Acta, v. 75, no. 16, p. 4416–4425, doi: 10.1016/j.gca.2011.05.004.

Tripati, A.K., Hill, P.S., Eagle, R.A., Mosenfelder, J.L., Tang, J., Schauble, E.A., Eiler, J.M., Zeebe, R.E., Uchikawa, J., Coplen, T.B., Ries, J.B., and Henry, D., 2015, Beyond temperature: Clumped isotope signatures in dissolved inorganic carbon species and the influence of solution chemistry on carbonate mineral composition: Geochimica et Cosmochimica Acta, v. 166, p. 344–371, doi: 10.1016/j.gca.2015.06.021.

Weinkauf, M.F.G., Kunze, J.G., Waniek, J.J., and Kučera, M., 2016, Seasonal Variation in Shell Calcification of Planktonic Foraminifera in the NE Atlantic Reveals Species-Specific Response to Temperature, Productivity, and Optimum Growth Conditions: PLOS ONE PLoS ONE, v. 11, no. 2, doi: 10.1371/journal.pone.0148363.

Zaarur, S., Olack, G., and Affek, H.P., 2011, Paleo-environmental implication of clumped isotopes in land snail shells: Geochimica et Cosmochimica Acta, v. 75, no. 22, p. 6859–6869, doi: 10.1016/j.gca.2011.08.044.

Zaarur, S., Affek, H.P., and Brandon, M.T., 2013, A revised calibration of the clumped isotope thermometer: Earth and Planetary Science Letters, v. 382, p. 47–57, doi: 10.1016/j.epsl.2013.07.026.

7. Appendix

Table A1

Sample	Description	Growth Temp (WOA Estimate) (^{o}C)	Growth Temp ($\delta^{18}O_{carbonate}$) (^{o}C)	Δ_{47} (Ghosh)
V23-22	Bulk-This Study	10.7	9.9	0.706
CHN43-109	Bulk-This Study	16.7	16.5	0.672
V31-134	Bulk-This Study	25.7	23.3	0.652
Pulleniatina obliquiloculata	Tripati et al. (2010)	23	23	0.655
Globigerinoides ruber	Tripati et al. (2010)	24.5	24.5	0.658
Globigerinoides ruber	Tripati et al. (2010)	24	24	0.638
Globigerinoides ruber	Tripati et al.(2010)	23.5	23.5	0.654
Globigerinoides ruber	Tripati et al. (2010)	29.2	29.2	0.625
Globigerinoides ruber	Tripati et al. (2010)	29.2	29.2	0.628
Globigerinoides ruber	Tripati et al. (2010)	29.2	29.2	0.627
Globigerinoides sacculifer	Tripati et al. (2010)	29.2	29.2	0.637
Globigerinoides sacculifer	Tripati et al. (2010)	27	27.1	0.634
Globigerinoides sacculifer	Tripati et al. (2010)	28	25.7	0.643
Globigerinoides sacculifer	Tripati et al. (2010)	23.5	25.7	0.658
Globigerinoides sacculifer	Tripati et al. (2010)	22	25.4	0.668
Globigerinoides sacculifer	Tripati et al. (2010)	26.8	28.2	0.644
Globigerinoides sacculifer	Tripati et al. (2010)	21	28.8	0.657
Globigerina bulloides	Tripati et al. (2010)	14.7	12.9	0.697
Globigerina bulloides	Tripati et al. (2010)	9.1	9.2	0.723
C. pachyderma	Grauel et al. (2013)	6	8.9	0.749
G. inflata	Grauel et al. (2013)	17	16.4	0.648
G. inflata	Grauel et al. (2013)	14.5	13.1	0.673
G. ruber (white)	Grauel et al. (2013)	18.5	21.4	0.696

G. ruber (white)	Grauel et al. (2013)	20.3	19.3	0.669
G. ruber (white)	Grauel et al. (2013)	18.2	20.1	0.667
G. ruber (white)	Grauel et al. (2013)	21.8	21	0.701
G. ruber (white)	Grauel et al. (2013)	19	21.9	0.666
G. ruber (white)	Grauel et al. (2013)	19	21.6	0.645
G. ruber (white)	Grauel et al. (2013)	19	21.7	0.664
G. ruber (white)	Grauel et al. (2013)	19	23.1	0.675
G. ruber (white)	Grauel et al. (2013)	19	23.2	0.663
G. ruber (white)	Grauel et al. (2013)	22.5	22.2	0.669
G. ruber (white)	Grauel et al. (2013)	22.2	22.5	0.658
G. ruber (white)	Grauel et al. (2013)	26	28.6	0.632
G. ruber (white)	Grauel et al. (2013)	26.1	27.3	0.644
G. ruber (white)	Grauel et al. (2013)	26.2	28.5	0.649
G. ruber (white)	Grauel et al. (2013)	26.2	27.1	0.661
G. ruber (white)	Grauel et al. (2013)	26.3	24.6	0.651
G. ruber (white)	Grauel et al. (2013)	26.3	27.6	0.634
G. ruber (white)	Grauel et al. (2013)	26.3	27.1	0.635
G. ruber (white)	Grauel et al. (2013)	27.5	28.8	0.65
G. ruber (white)	Grauel et al. (2013)	28.1	29	0.636
G. ruber (white)	Grauel et al. (2013)	28	29.6	0.628
G. truncatulinoides	Grauel et al. (2013)	14	15.3	0.665
G. truncatulinoides	Grauel et al. (2013)	14.9	15.6	0.685
N. pachyderma (sin)	Grauel et al. (2013)	5.5	1.5	0.737
N. pachyderma (sin)	Grauel et al. (2013)	2	3.7	0.72
N. pachyderma (sin)	Grauel et al. (2013)	2	2.1	0.73
N. pachyderma (sin)	Grauel et al. (2013)	2	1.8	0.777
O. universa	Grauel et al. (2013)	18.5	19.8	0.675
O. universa	Grauel et al. (2013)	20.3	16.2	0.681
O. universa	Grauel et al. (2013)	21.5	19.9	0.669
O. universa	Grauel et al. (2013)	18.2	20.1	0.66
O. universa	Grauel et al. (2013)	18.2	17.6	0.666
O. universa	Grauel et al. (2013)	20.5	19.3	0.68
O. universa	Grauel et al. (2013)	21.8	21.9	0.67
O. universa	Grauel et al. (2013)	19.1	17.3	0.661
O. universa	Grauel et al. (2013)	22.5	22.1	0.668
O. universa	Grauel et al. (2013)	22.2	21.5	0.662

U. mediterranea	Grauel et al. (2013)	13.9	17.3	0.687
U. mediterranea	Grauel et al. (2013)	13.9	17.1	0.704

Table 2A

High Latitude	
Species	**Depth Habitat**
Globigerina bulloides	Mixed Layer
Globoconella inflata	Thermocline
Hirsutella scitula	Subthermocline
Neogloboquadrina pachyderma	Thermocline
Truncorotalia truncatulinoides	Subthermocline
Neogloboquadrina incompta	Thermocline
Tropical/Subtropical	
Species	**Depth Habitat**
Orbulina universa	Mixed Layer
Globigerinella calida	Thermocline
Globigerinoides conglobatus	Mixed Layer
Globorotaloides hexagonus	Subthermocline
Globigerinoides ruber pink	Mixed Layer
Globigerinoides ruber white	Mixed Layer
Globigerinoides sacculifer	Mixed Layer
Globoturborotalita rubescens	Mixed Layer
Globorotalia tumida	Subthermocline
Globorotalia ungulata	Thermocline
Hirsutella hirsuta	Subthermocline
Menardella menardii	Thermocline
Neogloboquadrina dutertrei	Thermocline
Pulleniatina obliquiloculata	Thermocline
Truncorotalia truncatulinoides	Subthermocline